



# Sirtuin 2 Isoform 1 Enhances Hepatitis B Virus RNA Transcription and DNA Synthesis through the AKT/GSK-3 $\beta$ / $\beta$ -Catenin Signaling Pathway

Zahra Zahid Piracha,<sup>a,b</sup> Hyeonjoong Kwon,<sup>a,b</sup> Umar Saeed,<sup>a,b</sup> Jumi Kim,<sup>a,b</sup> Jaesung Jung,<sup>a,b\*</sup> Yong-Joon Chwae,<sup>a,b</sup> Sun Park,<sup>a,b</sup> Ho-Joon Shin,<sup>a,b</sup> Kyongmin Kim<sup>a,b</sup>

<sup>a</sup>Department of Microbiology, Ajou University School of Medicine, Suwon, South Korea

<sup>b</sup>Department of Biomedical Science, Graduate School of Ajou University, Suwon, South Korea

**ABSTRACT** Sirtuin 2 (Sirt2), a NAD<sup>+</sup>-dependent protein deacetylase, is overexpressed in many hepatocellular carcinomas (HCCs) and can deacetylate many proteins, including tubulins and AKT, prior to AKT activation. Here, we found that endogenous Sirt2 was upregulated in wild-type hepatitis B virus (HBV WT)-replicating cells, leading to tubulin deacetylation; however, this was not the case in HBV replication-deficient-mutant-transfected cells and 1.3-mer HBV WT-transfected and reverse transcriptase inhibitor (entecavir or lamivudine)-treated cells, but all HBV proteins were expressed. In HBV WT-replicating cells, upregulation of Sirt2 induced AKT activation, which consequently downregulated glycogen synthase kinase 3 $\beta$  (GSK-3 $\beta$ ) and increased  $\beta$ -catenin levels; however, downregulation of Sirt2 in HBV-nonreplicating cells impaired AKT/GSK-3 $\beta$ / $\beta$ -catenin signaling. Overexpression of Sirt2 isoform 1 stimulated HBV transcription and consequently HBV DNA synthesis, which in turn activated AKT and consequently increased  $\beta$ -catenin levels, possibly through physical interactions with Sirt2 and AKT. Knockdown of Sirt2 by short hairpin RNAs (shRNAs), inhibition by 2-cyano-3-[5-(2,5-dichlorophenyl)-2-furanyl]-N-5-quinoliny-2-propenamide (AGK2), or dominant negative mutant expression inhibited HBV replication, reduced AKT activation, and decreased  $\beta$ -catenin levels. Through HBV infection, we demonstrated that Sirt2 knockdown inhibited HBV replication from transcription. Although HBx itself activates AKT and upregulates  $\beta$ -catenin, Sirt2-mediated signaling and upregulated HBV replication were HBx independent. Since constitutively active AKT inhibits HBV replication, the results suggest that upregulated Sirt2 and activated AKT may balance HBV replication to prolong viral replication, eventually leading to the development of HCC. Also, the results indicate that Sirt2 inhibition may be a new therapeutic option for controlling HBV infection and preventing HCC.

**IMPORTANCE** Even though Sirt2, a NAD<sup>+</sup>-dependent protein deacetylase, is overexpressed in many HCCs, and overexpressed Sirt2 promotes hepatic fibrosis and associates positively with vascular invasion by primary HCCs through AKT/GSK-3 $\beta$ / $\beta$ -catenin signaling, the relationship between Sirt2, HBV, HBx, and/or HBV-associated hepatocarcinogenesis is unclear. Here, we show that HBV DNA replication, not HBV expression, correlates positively with Sirt2 upregulation and AKT activation. We demonstrate that overexpression of Sirt2 further increases HBV replication, increases AKT activation, downregulates GSK-3 $\beta$ , and increases  $\beta$ -catenin levels. Conversely, inhibiting Sirt2 decreases HBV replication, reduces AKT activation, and decreases  $\beta$ -catenin levels. Although HBx activates AKT to upregulate  $\beta$ -catenin, Sirt2-mediated effects were not dependent on HBx. The results also indicate that a Sirt2 inhibitor may control HBV infection and prevent the development of hepatic fibrosis and HCC.

**KEYWORDS** HBV replication, Sirt2 isoform 1

**Received** 31 May 2018 **Accepted** 9 August 2018

**Accepted manuscript posted online** 15 August 2018

**Citation** Piracha ZZ, Kwon H, Saeed U, Kim J, Jung J, Chwae Y-J, Park S, Shin H-J, Kim K. 2018. Sirtuin 2 isoform 1 enhances hepatitis B virus RNA transcription and DNA synthesis through the AKT/GSK-3 $\beta$ / $\beta$ -catenin signaling pathway. *J Virol* 92:e00955-18. <https://doi.org/10.1128/JVI.00955-18>.

**Editor** J.-H. James Ou, University of Southern California

**Copyright** © 2018 American Society for Microbiology. All Rights Reserved.

Address correspondence to Kyongmin Kim, kimkm@ajou.ac.kr.

\* Present address: Jaesung Jung, Mogam Biotechnology Institute, Yongin, South Korea.

Hepatitis B virus (HBV) infection can cause acute and chronic hepatitis, cirrhosis, and primary hepatocellular carcinoma (HCC). Chronic infection with HBV is a major health problem worldwide, even though an effective vaccine is available. HBV belongs to the *Hepadnaviridae* family and has a 3.2-kbp, partially double-stranded, relaxed circular (RC) DNA genome (1). The virus has a specific tropism for liver cells; i.e., it is hepatotropic. The HBV life cycle has been studied extensively, but the host factors involved in HBV replication and the mechanisms underlying HBV-associated HCC are not completely understood. During the HBV life cycle, viral infection of hepatocytes occurs through binding to heparan sulfate, followed by the sodium taurocholate cotransporting polypeptide (NTCP) receptor for virion entry (2). This is followed by uncoating of the envelope and transport of the core particle (capsid or nucleocapsid) through microtubules to the perinuclear region and finally to the nuclear pore complex (NPC) (3). Upon reaching the NPC, the core particle dissociates and releases the partially double-stranded RC DNA genome, which is then converted to covalently closed circular DNA (cccDNA) (4). The cccDNA acts as a minichromosome and as a template for transcription of viral genes. Viral transcripts, mainly 3.5, 2.4, 2.1, and 0.7 kb in size, are produced from this viral minichromosome and then transported to the cytoplasm, where they are translated to produce viral proteins, namely, viral surface (HBs or S), core (HBc or C), viral polymerase (P), and X (HBx) proteins (5). HBs includes large HBs (LHBs), middle HBs (MHBs), and small HBs (SHBs). HBx, a HBV oncoprotein, plays a role in the development of HCC (6).

The histone deacetylase (HDAC) superfamily comprises a vast array of enzymes in prokaryotes and mammals; these enzymes regulate posttranslational modification. Mammalian HDACs are classified into four families: classes I, IIa, IIb, and IV. In addition to these classical HDACs, there is another group of HDACs, called sirtuins (Sirts), which are sometimes classified as atypical class III HDACs (7). The mammalian Sirt family proteins (Sirt1 to Sirt7) are homologs of the yeast silent information regulator 2 (Sir2) protein and require NAD (NAD<sup>+</sup>) as a cofactor (cosubstrate) for their protein deacetylase activity at acetylated lysine residues (8, 9). In yeast, Sir2 regulates aging by maintaining transcriptional silencing of the mating-type loci, the ribosomal DNA locus, and the telomeres (10). Among the seven Sirts, Sirt1, Sirt2, and Sirt3 are closely related and classified as class I Sirts; they are localized mainly to the nucleus, cytoplasm, and mitochondria, respectively (11). Sirt1, Sirt2, and Sirt3 are involved in HBV infection: Sirt1 is recruited to the HBV cccDNA minichromosome to increase HBV transcription and replication (12), whereas Sirt3 inhibits HBV replication by reducing cellular levels of reactive oxygen species (13). Sirt2 proteins aggravate posts ischemic liver injury (14), may induce hepatic fibrogenesis through the Sirt2/extracellular signal-regulated kinase (ERK)/c-myc pathway (15), and are overexpressed in many HCCs (16, 17). Recently, it was reported that HBx upregulates Sirt2 expression and that Sirt2 has a positive role in HBV replication and HBV-induced HCC (18).

Sirt2 substrates include  $\alpha$ -tubulin, histone H4K16, p53, FOXO3, and p65 (9, 19–21). Sirt2 is active mainly in the cytoplasm, where it deacetylates  $\alpha$ -tubulin in microtubules (22). Deficiency of Sirt2 causes mitotic cell death and a high tendency toward the development of gender-specific tumors (23). Also, Sirt2 expression is downregulated in gliomas (24). These contradictory roles in different tumors suggest that Sirt2 may have a dual function as a tumor suppressor (23, 24) and progressor (16, 17).

Sirt2 interacts physically with AKT (protein kinase B [PKB]), which is critical for complete activation of AKT (25). For complete AKT activation, deacetylation by Sirt2 is also required (16). AKT, a downstream target of phosphatidylinositol 3-kinase (PI3K), is a main component in the signal transduction pathway that regulates a number of cellular processes, including proliferation, differentiation, and survival (26). The PI3K/AKT pathway is regulated by growth factors that activate PI3K, which in turn phosphorylates phosphatidylinositol-4,5-bisphosphate (PIP2) to form phosphatidylinositol-3,4,5-trisphosphate (PIP3). PIP3 acts as a docking site for AKT and facilitates the subsequent phosphorylation of AKT at threonine 308 (pT308) by phosphoinositide-dependent kinase 1. Complete activation of AKT also requires phosphorylation at serine 473

(pS473) (27, 28). It is generally believed that the activation of the PI3K-AKT pathway by viruses inhibits apoptosis and promotes the survival of infected cells to favor viral replication (29, 30).

Even though it has been shown that Sirt2 increases HBV replication (18), the underlying signaling mechanism and the effects of HBV expression and/or DNA synthesis on Sirt2 expression have not been investigated in detail. Here, we examined the effects of Sirt2 isoform 1 (Sirt2.1) on HBV transcription and replication. The results showed that HBV replication upregulates Sirt2, but replication-deficient HBV mutant expression impairs Sirt2 activity. We also demonstrated that overexpression of Sirt2 further promotes HBV transcription and replication, which are independent of HBx, and that inhibition or knockdown of Sirt2 inhibits HBV transcription and replication. Furthermore, the results highlight the importance of the Sirt2-mediated AKT/glycogen synthase kinase 3 $\beta$  (GSK-3 $\beta$ )/ $\beta$ -catenin signaling pathway for HBV replication. Finally, we suggest that Sirt2 may be a new therapeutic target for controlling HBV infection and preventing progression to HCC.

## RESULTS

**HBV replication upregulates endogenous Sirt2, leading to deacetylation of  $\alpha$ -tubulin.** Viruses modify the host environment to suit their own requirements and complete the life cycle. Viruses control the cellular gene transcription machinery either to activate genes that help them or to repress those that are hostile. Acetylation is an important phenomenon that controls gene transcription; hence, it is speculated that viruses control this signaling pathway (31). Several viral proteins interact with histone acetyltransferases and histone deacetyltransferases to disrupt cellular acetylation signaling pathways (31). Similarly, acetylation of  $\alpha$ -tubulin is linked to early fusion of human immunodeficiency virus (HIV) (32). HDAC6 inhibits influenza virus replication by negatively regulating the assembly of viral components at the site of replication via acetylated microtubules (33). For efficient infection, as well as for early steps of hepatitis C virus (HCV) infection, a dynamic microtubule structure is required (34).

To determine the acetylation status of  $\alpha$ -tubulin during the HBV life cycle, we examined  $\alpha$ -tubulin acetylation in HBV-replicating HCC cells (i.e., stable HBV-expressing HepAD38 [35] and HepG2.2.15 [36] cells) and in Huh7 cells transiently transfected with wild-type HBV (HBV WT) in which replicative intermediate (RI) DNAs, including HBV RC, double-stranded linear (DL), and single-stranded (SS) DNAs, are synthesized (Fig. 1A, bottom panel, lanes 2, 4, and 6). The level of acetylation of  $\alpha$ -tubulin in cells containing replicating HBV was lower than that in the respective nonreplicating or mock controls (Fig. 1A, top panel, lane 1 versus 2, lane 3 versus 4, and lane 5 versus 6). Of note, the  $\alpha$ -tubulin level was constant (Fig. 1A, second panel). Since Sirt2 is a cytoplasmic  $\alpha$ -tubulin deacetylase (22), endogenous Sirt2 mRNA and protein expressions were examined by Northern and Western blot analyses, respectively. The results showed that Sirt2 mRNA and protein expressions were upregulated when HBV was replicating (Fig. 1A, third and seventh panels, lanes 2, 4, and 6).

To determine whether  $\alpha$ -tubulin deacetylation and upregulated Sirt2 expression are linked to HBV DNA synthesis or HBV expression, we transfected Huh7 cells with HBV WT or replication-deficient TP-Y65F or RT-YMHA mutants. HBV TP-Y65F, a protein-priming reaction-deficient mutant, initiates minus-strand DNA without a primer, thereby synthesizing the short oligomer TGAA or GAA (the nascent minus-strand DNA); however, oligomer translocation and HBV minus-strand DNA elongation cannot occur, making the virus replication deficient (37). The presence of HBV RT-YMHA, the conserved reverse transcriptase (RT) active YMDD motif in YMHA mutants, results in a RT-deficient, dead virus that does not support HBV DNA synthesis *in vivo* (37, 38). Hence, TP-Y65F and RT-YMHA mutants show HBV RNA (Fig. 1B, eighth panel) and HBc protein (Fig. 1B, fourth panel) expression, core particle formation (Fig. 1B, fifth panel), and pregenomic RNA (pgRNA) encapsidation (Fig. 1B, sixth panel) but cannot synthesize HBV RI DNAs (Fig. 1B, seventh panel, lane 2 versus 3 and 4) (37). It should be mentioned here that HBV pgRNAs of the WT and replication-deficient mutants are expressed under the

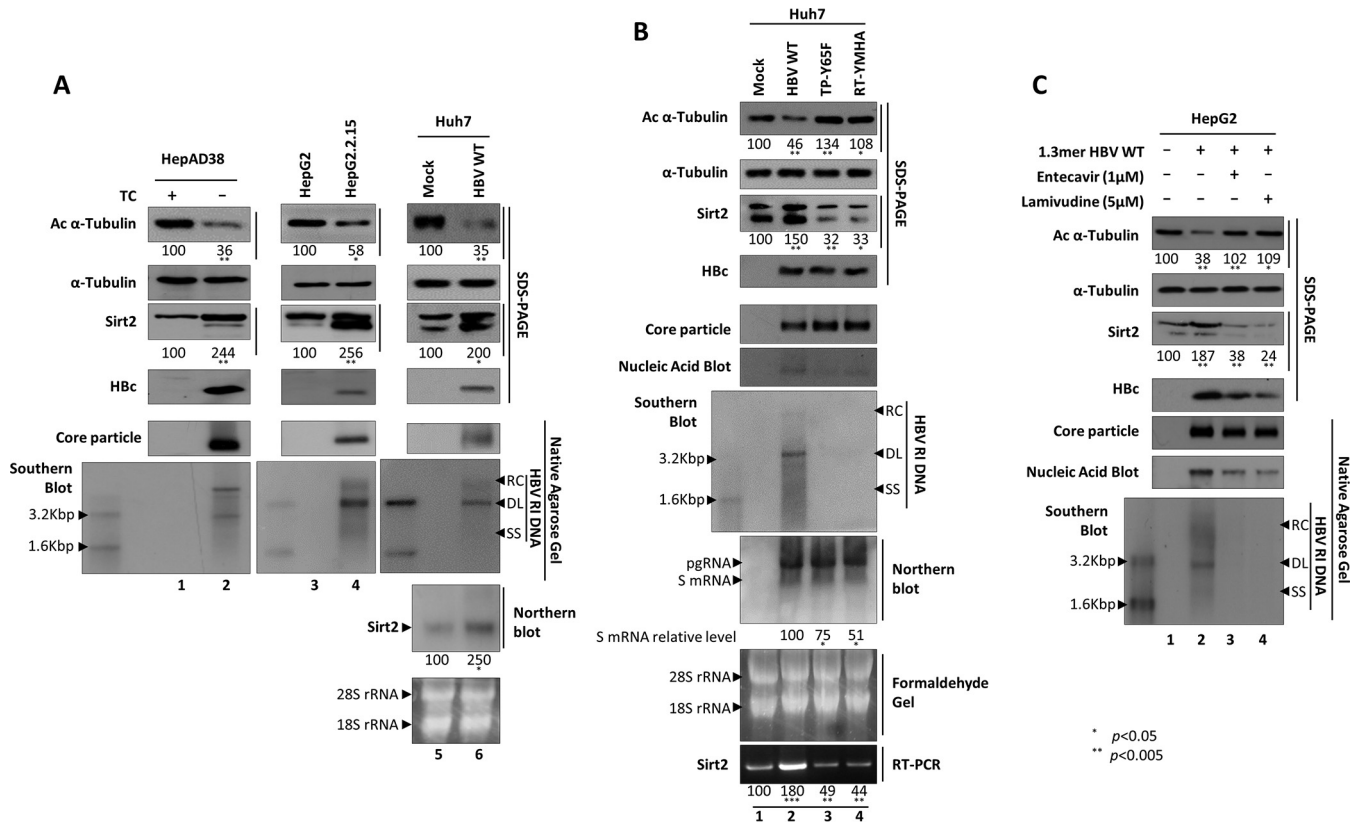


**FIG 1** Sirt2 is upregulated and  $\alpha$ -tubulin is deacetylated in HBV WT-replicating cells but not in HBV replication-deficient mutant-expressing cells. (A) Association between  $\alpha$ -tubulin deacetylation and Sirt2 expression in HBV-replicating stable HepAD38, HepG2.2.15, and HBV WT ( $4 \mu$ g)-transfected Huh7 cells. HepAD38 and tetracycline (TC)-removed HepAD38 cells (lanes 1 and 2), newly plated HepG2 and HepG2.2.15 cells (lanes 3 and 4), and transiently mock- and HBV WT-transfected Huh7 cells (lanes 5 and 6) were cultured for 72 h. (B)  $\alpha$ -Tubulin deacetylation and Sirt2 expression in HBV WT- and replication-deficient mutant-transfected Huh7 cells. At 72 h posttransfection, lysates were prepared from mock (lane 1)-, HBV WT (lane 2)-, TP-Y65F mutant (lane 3)-, and RT-YMHA mutant (lane 4)-transfected Huh7 cells. (C)  $\alpha$ -Tubulin deacetylation and Sirt2 expression in RT inhibitor-treated HBV WT-transfected HepG2 cells. The 1.3-mer HBV WT-transfected HepG2 cells were mock treated (lane 2) or treated with 1  $\mu$ M entecavir (lane 3) or 5  $\mu$ M lamivudine (lane 4) at 24 h posttransfection for 48 h. Lane 1 shows mock-transfected HepG2 cell. SDS-PAGE and Western blotting (first to fourth panels) and native agarose gel electrophoresis and Western blotting (fifth panel) were performed to detect proteins and core particle formation, respectively (A to C). *In situ* nucleic acid blotting (B and C, sixth panels) was performed to detect all of the nucleic acids inside core particles. Southern and Northern blot analyses were performed to reveal HBV DNA synthesis (A to C, bottom, seventh, and bottom panels, respectively), HBV total RNA levels (B, eighth and bottom panels), and Sirt2 RNA levels (A, seventh and bottom panels, lanes 5 and 6), respectively. Acetylated (Ac)  $\alpha$ -tubulin,  $\alpha$ -tubulin, endogenous Sirt2, and Hbc proteins were detected using monoclonal anti-acetylated tubulin clone 6-11B-1 (1:1,000) (catalog number T 6793; Sigma-Aldrich), mouse monoclonal anti- $\alpha$ -tubulin (TU-02) (1:5,000) (catalog number sc-8035; Santa Cruz), polyclonal rabbit anti-Sirt2 (H-95) (1:1,000) (catalog number sc-20966; Santa Cruz), and polyclonal rabbit anti-Hbc (1:1,000) (75) antibodies, respectively. Tubulin was used as a loading control. For core particle formation, core particles on PVDF membranes were incubated with a polyclonal rabbit anti-Hbc (1:1,000) (75) antibody. For Southern blotting, HBV DNA extracted from isolated core particles was separated, transferred to a nylon membrane, hybridized with a random-primed  $^{32}$ P-labeled full-length HBV-specific probe, and subjected to autoradiography. HBV replicative intermediate, single-stranded, double-stranded linear, and partially double-stranded relaxed circular DNAs are marked as HBV RI DNA, SS, DL, and RC, respectively. For *in situ* nucleic acid blotting, isolated core particles on PVDF membranes were treated with 0.2 N sodium hydroxide, hybridized, and subjected to autoradiography. For Northern blotting, 20  $\mu$ g of total RNA was separated by 1% formaldehyde gel electrophoresis, transferred to nylon membranes, hybridized, and subjected to autoradiography as described above for Southern blotting. The 3.5-kb pgRNA and the 2.1- and 2.4-kb mRNAs encoding the S protein are indicated. For the Sirt2 mRNA level, RT-PCR was performed. Relative levels of acetylated  $\alpha$ -tubulin, endogenous Sirt2, and 2.4- and 2.1-kb S mRNAs were measured using ImageJ 1.46r. Data represent the mean levels of acetylated  $\alpha$ -tubulin, Sirt2, and S mRNA from three independent experiments. Statistical significance was evaluated using Student's *t* test. *P* values relative to the respective control are shown.

control of the cytomegalovirus immediate early (CMV IE) promoter, and subgenomic mRNAs are expressed under the control of their authentic promoters (Fig. 1B, eighth panel) (37). Consistent with the data in Fig. 1A (third panel), Sirt2 mRNA and protein expressions were upregulated markedly when HBV DNA was synthesized in HBV WT-transfected cells (Fig. 1B, third and bottom panels, lane 2); however, Sirt2 mRNA and protein levels were downregulated markedly in HBV replication-deficient mutant-transfected cells (Fig. 1B, third and bottom panels, lanes 3 and 4). Accordingly,  $\alpha$ -tubulin was deacetylated in HBV WT-transfected cells when HBV DNA was synthesized (Fig. 1B, top panel, lane 2), whereas  $\alpha$ -tubulin was deacetylated to a lesser extent in HBV replication-deficient mutant-transfected cells than in mock-transfected cells

(Fig. 1B, top panel, lane 1 versus 3 and 4). Of particular note, replication-deficient mutant-transfected cells have more-decreased S mRNA levels than those of HBV WT-transfected cells (Fig. 1B, eighth panel, lane 2 versus 3 and 4).

To further strengthen the above-mentioned observation that  $\alpha$ -tubulin deacetylation and upregulated Sirt2 expression are associated with HBV DNA synthesis, 1.3-mer HBV WT-transfected HepG2 cells were treated with a RT inhibitor, entecavir (1  $\mu$ M) or lamivudine (5  $\mu$ M), to inhibit HBV DNA synthesis from 24 to 72 h posttransfection (Fig. 1C, bottom panel, lane 2 versus 3 and 4) (39, 40). The results of an MTT [3-(4,5-dimethylthiazol-2-yl)-2,5-diphenyltetrazolium bromide] assay revealed that neither entecavir nor lamivudine was cytotoxic (data not shown). Consistent with the data in Fig. 1B, Sirt2 expression was markedly downregulated and  $\alpha$ -tubulin was deacetylated to a lesser extent in entecavir- or lamivudine-treated cells than in mock-transfected cells (Fig. 1C, top and third panels, lane 1 versus 3 and 4). This demonstrates that HBV replication increases Sirt2 expression, leading to  $\alpha$ -tubulin deacetylation; however, HBV expression or RT inhibitor treatment without DNA synthesis inhibits Sirt2 expression, leading to  $\alpha$ -tubulin acetylation.

**Overexpression of Sirt2 isoform 1 upregulates HBV replication.** Figure 1 shows that HBV DNA synthesis is closely related to the upregulation of Sirt2 and deacetylation of  $\alpha$ -tubulin. Five splice variants of the human SIRT2 gene were identified (GenBank accession numbers [NP\\_036369](#), [NP\\_085096](#), [NP\\_001180215](#), [NR\\_034146.1](#), and [KF032391](#)). Among these, transcript variants 1 and 2 encode proteins of physiological relevance, so-called isoform 1 (Sirt2.1) and isoform 2 (Sirt2.2), respectively (Fig. 2A) (41). Sirt2 isoform 5 (Sirt2.5) (Fig. 2A) is localized to the nucleus and lacks deacetylase activity toward known Sirt2 substrates (42). Since both Sirt2 and HDAC6 have  $\alpha$ -tubulin deacetylase activity (22), we obtained cytoplasmic and nuclear fractions from lysates of HEK293T cells transfected with constructs containing isoforms of Sirt2 or HDAC6 (Fig. 2B). Sirt2.1, Sirt2.2, and Sirt2.5 (3 $\times$ FLAG tagged) and HDAC6 (MYC tagged) were identified by sodium dodecyl sulfate-polyacrylamide gel electrophoresis (SDS-PAGE) and Western blotting at 72 h posttransfection. Since HDAC6 is an exclusively cytoplasmic protein (43), it was detected only in the cytoplasmic fraction (Fig. 2B, lane 5 versus 10). Sirt2.1 was expressed mostly in the cytoplasm (even at 72 h posttransfection); however, Sirt2.2 and Sirt2.5 accumulated in the cytoplasm and nucleus (Fig. 2B and data not shown) (42). Given that Sirt2 is overexpressed in HBV-replicating cells, leading to  $\alpha$ -tubulin deacetylation (Fig. 1), and Sirt2.1 is a major cytoplasmic protein (Fig. 2B) (42, 44), we focused on Sirt2.1 in this study.

To examine the effects of Sirt2.1 on HBV replication, we transiently cotransfected HepG2 (Fig. 2C, lanes 1 to 3) and Huh7 (Fig. 2C, lanes 4 to 6) cells with 1.3-mer HBV WT or with Sirt2.1 plus 1.3-mer HBV WT. Consistent with the results shown in Fig. 1, transfection of cells with the 1.3-mer HBV WT resulted in a marked reduction in  $\alpha$ -tubulin acetylation (Fig. 2C, top panel, lanes 2 and 5). When Sirt2.1 was overexpressed,  $\alpha$ -tubulin was deacetylated to an even greater extent (Fig. 2C, top panel, lanes 3 and 6). Also, HBs (LHBs, MHBs, and SHBs) protein levels, HBc protein levels, levels of core particle formation, and levels of HBV DNA synthesis in cells cotransfected with Sirt2.1 and the 1.3-mer HBV WT were significantly higher than those in cells transfected with the 1.3-mer HBV WT (Fig. 2C, lane 2 versus 3 and lane 5 versus 6), demonstrating that overexpression of Sirt2.1 upregulates HBV replication.

**Overexpression of Sirt2.1 increases HBV transcriptional activity.** We reasoned that the upregulated expression of HBc and HBs proteins in Sirt2.1-overexpressing cells was due to increased transcriptional activity of HBV, because all HBV mRNAs, including the pgRNA, are expressed under the control of their authentic promoters in 1.3-mer HBV WT-transfected cells. Therefore, to examine the effect of Sirt2.1 overexpression on HBV promoter activity, we performed a luciferase reporter assay in Huh7 and HepG2 cells (Fig. 3A). Upon Sirt2.1 overexpression, the promoter activities of all HBV enhancers and promoters (enhancer 1/X promoter [EnhI/Xp], enhancer 2/Core promoter [EnhII/ Cp], preS1p, and preS2p) was upregulated (Fig. 3A).

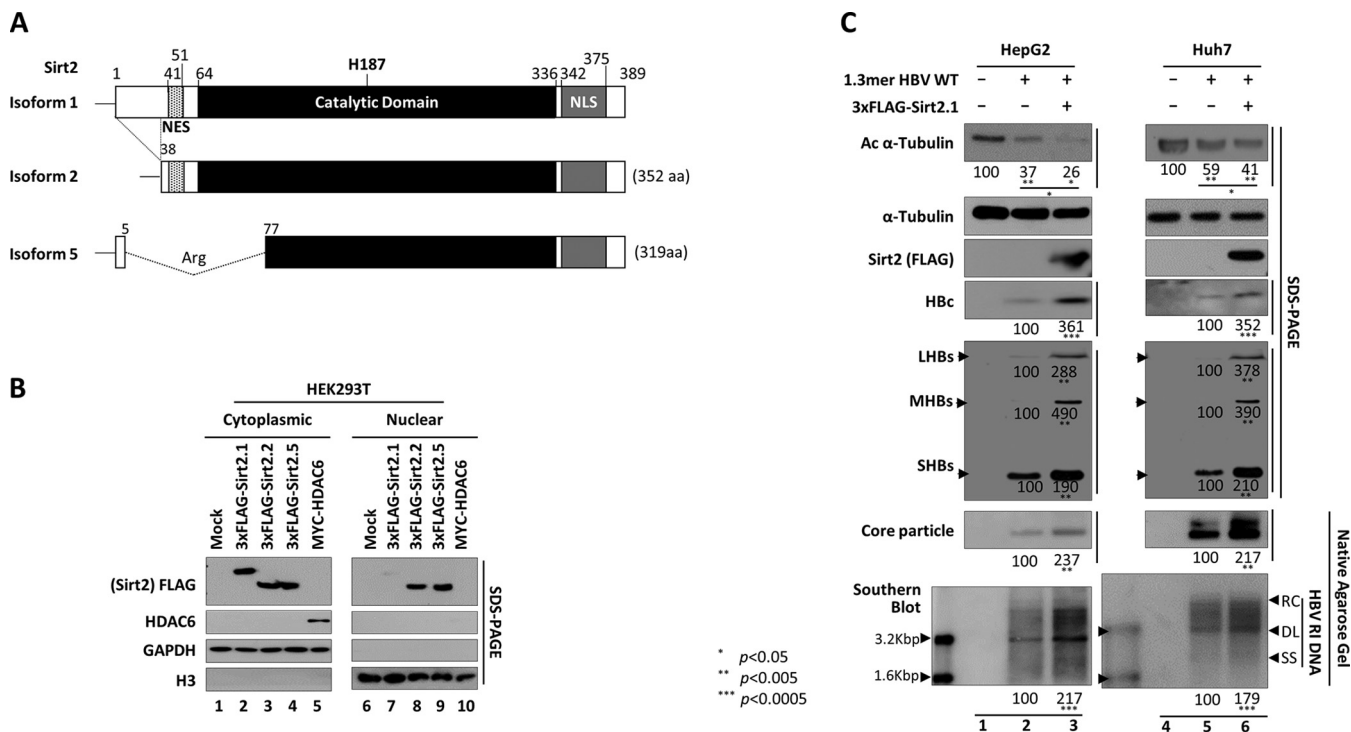


**FIG 2** Overexpression of Sirt2.1 increases HBV replication. (A) Schematic diagram of the three isoforms of Sirt2 obtained through splicing of the Sirt2 primary transcript. Residues are numbered according to isoform 1. The nuclear export signal (NES) (dotted), the catalytic domain (black), the nuclear localization signals (NLS) (gray), and the catalytically active H187 residue in the catalytic domain are indicated. Alternative splicing of Sirt2 pre-mRNA yields three distinct proteins: isoforms 1, 2, and 5. Sirt2 isoform 2 is 37 amino acid (aa) residues shorter than isoform 1. In the case of isoform 5, amino acids 6 to 76 are spliced out and replaced by an arginine (CGT) residue, resulting in the removal of the NES. (B) Three isoforms of Sirt2 obtained from cytoplasmic and nuclear fractions. HEK293T cells were transiently transfected with lanes 1 and 6) or transfected with 4  $\mu$ g of a plasmid encoding 3 $\times$ FLAG-tagged Sirt2 isoform 1 (lanes 2 and 7), isoform 2 (lanes 3 and 8), or isoform 5 (lanes 4 and 9) or HDAC6 (lanes 5 and 10). Cytoplasmic and nuclear fractions were prepared according to the manufacturer's instructions (Genetex). The cytoplasmic (lanes 1 to 5) and nuclear (lanes 6 to 10) fractions were examined by SDS-PAGE and Western blotting with the respective anti-FLAG, anti-HDAC6, anti-GAPDH, and anti-H3 antibodies. The purity of the cytoplasmic fraction was examined by testing for the presence of GAPDH and the absence of histone H3, and that of the nuclear fraction was examined by testing for the absence of GAPDH and the presence of histone H3. Monoclonal anti-FLAG M2 (1:1,000) (catalog number F1804; Sigma), rabbit polyclonal anti-H3 (1:5,000) (catalog number ab1791; Abcam), rabbit polyclonal anti-HDAC6 (1:1,000) (catalog number sc-11420; Santa Cruz), and mouse monoclonal anti-GAPDH (1:5,000) (catalog number sc-32233; Santa Cruz) were utilized. (C) Overexpression of Sirt2.1, an  $\alpha$ -tubulin deacetylase, increases HBV replication. HepG2 (lanes 1 to 3) and Huh7 (lanes 4 to 6) cells were mock transfected (lanes 1 and 4) or transiently transfected with 4  $\mu$ g of 1.3-mer HBV WT (ayw) (lanes 2 and 5) or with 4  $\mu$ g of a plasmid encoding 3 $\times$ FLAG-tagged Sirt2.1 construct (lanes 3 and 6), and lysates were prepared at 72 h posttransfection. The amount of transfected DNA was adjusted using pcDNA3. Rabbit polyclonal anti-HBs (1:1,000) (catalog number 1811; Virostat Inc.) was utilized. SDS-PAGE and Western blotting of proteins (first to fifth panels), native agarose gel electrophoresis and Western blotting of core particles (sixth panel), and Southern blotting for HBV DNA (bottom panel) were performed as described in the legend of Fig. 1. Relative levels of acetylated  $\alpha$ -tubulin; LHBs, MHBs, and SHBs proteins; HBc protein; core particles; and HBV DNA were measured using ImageJ 1.46r. Data are presented as mean values from three independent experiments. Statistical significance was evaluated using Student's *t* test. *P* values relative to the respective control are shown.

Since Sirt2.1 overexpression increases HBV promoter and enhancer activities (Fig. 3A), we performed Northern blotting of Huh7 or HepG2 cells cotransfected with the 1.3-mer HBV WT or Sirt2.1 plus the 1.3-mer HBV WT (Fig. 3B). HBV pgRNA and subgenomic S mRNA levels increased significantly in cells cotransfected with Sirt2.1 plus 1.3-mer HBV WT (Fig. 3B, lanes 3 and 6), demonstrating that Sirt2.1 overexpression upregulates HBV transcription, thereby increasing HBV replication.

**HBV replication is downregulated when Sirt2 is inhibited or knocked down.**

Since Sirt2.1 overexpression upregulates HBV replication via increased transcription of HBV pgRNA and mRNA (Fig. 3), we further examined whether inhibiting Sirt2 downregulates HBV replication. To examine the effect of Sirt2.1 inhibition on HBV replication, we exposed 1.3-mer HBV WT-transfected Huh7 (Fig. 4A) and HepG2 (see Fig. 8C and data not shown) cells to the potent Sirt2 inhibitor AGK2 (10  $\mu$ M) (45) from the time of transfection up until 72 h posttransfection. The results of an MTT assay revealed that AGK2 was not cytotoxic (data not shown). Levels of HBc protein expression, core particle formation, and HBV DNA synthesis fell significantly (Fig. 4A, lane 3). Inhibition

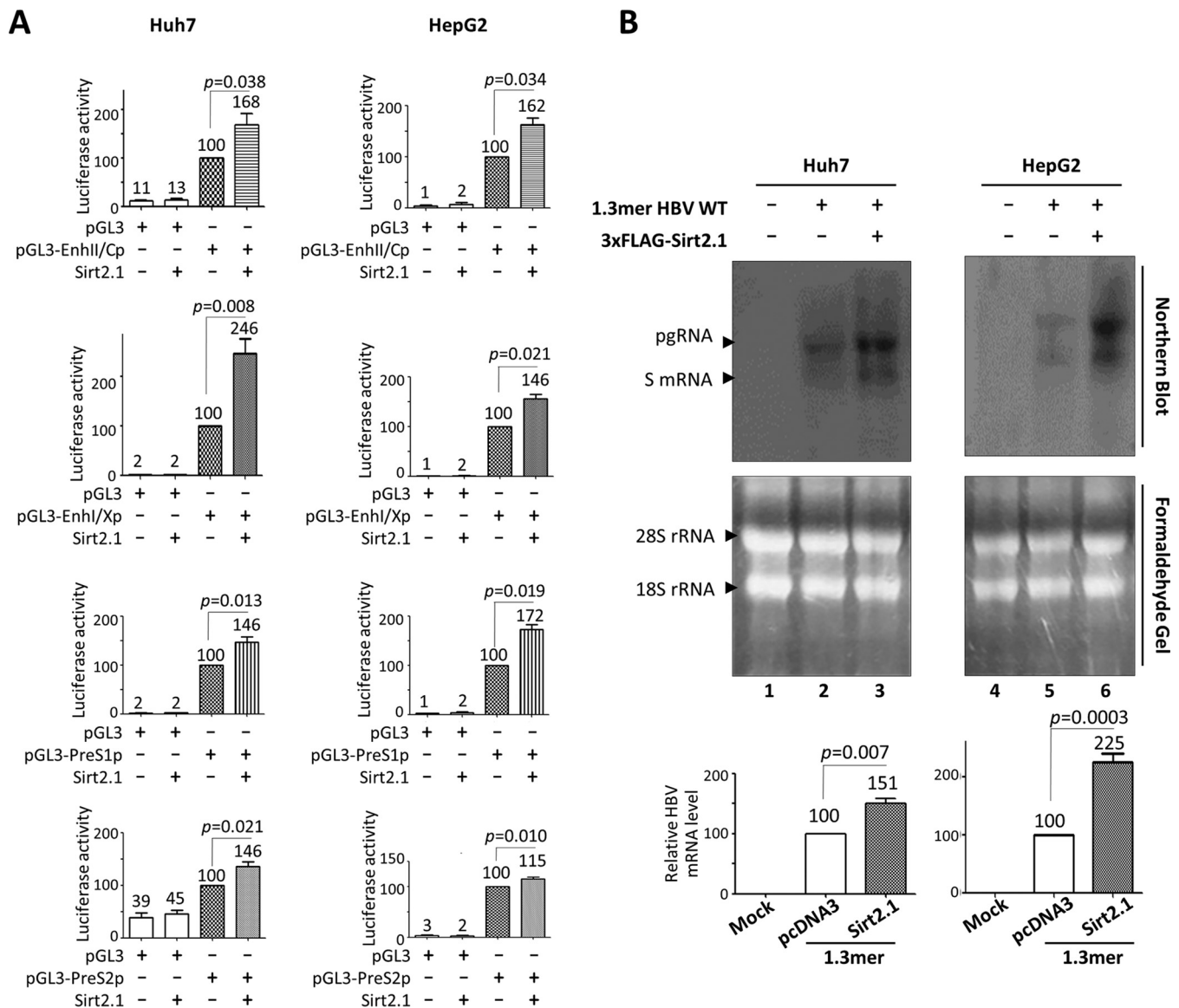


**FIG 3** Transcription of HBV RNA increases upon overexpression of Sirt2.1. (A) Luciferase reporter assays to detect HBV enhancer and promoter activities upon overexpression of Sirt2. Huh7 (first row) or HepG2 (second row) cells were transiently transfected with 2  $\mu$ g of the indicated luciferase reporter vectors in the presence or absence of 3 $\times$ FLAG-Sirt2.1 (2  $\mu$ g). The amount of transfected DNA was adjusted using pcDNA3. At 72 h posttransfection, lysates were prepared (catalog number E153A; Promega), and luciferase activity relative to the respective control luciferase reporter vector is presented. Data are expressed as the mean luciferase activities from four independent experiments. (B) Northern blotting to show increased expression of HBV mRNAs upon overexpression of Sirt2.1. Huh7 (lanes 1 to 3) and HepG2 (lanes 4 to 6) cells were transiently mock transfected (lanes 1 and 4) or transfected with 4  $\mu$ g of 1.3-mer HBV WT (ayw) (lanes 2 and 5) or 4  $\mu$ g of 1.3-mer HBV WT (ayw) plus 4  $\mu$ g of the 3 $\times$ FLAG-Sirt2.1 construct (lanes 3 and 6), and total RNA was harvested at 72 h posttransfection. The amount of transfected DNA was adjusted using pcDNA3. Northern blotting was performed as described in the legend of Fig. 1B. Data are presented as mean relative HBV mRNA levels from four independent experiments. Statistical significance was evaluated using Student's *t* test. Exact *P* values relative to the respective control are shown.

by the AGK2 inhibitor was fully effective, even in Sirt2.1-overexpressing cells (Fig. 4A, lane 5). The amount of  $\alpha$ -tubulin deacetylation also fell accordingly (Fig. 4A, top panel, lanes 3 and 5).

Since AGK2 treatment reduced HBV replication (Fig. 4A), we also examined the effect of knocking down Sirt2 (using a lentiviral short hairpin RNA [shRNA] system) on HBV replication. Huh7 and HepG2 cells transduced with lentiviral control shRNA (shControl) or Sirt2 shRNAs (shSIRT2-#1 to -#4) were transfected with the 1.3-mer HBV WT (Fig. 4B, lane 3 versus 4 to 7 and lane 10 versus 11 to 14). Sirt2 knockdown (KD) cells showed reduced Sirt2 expression (Fig. 4B, third panel, lanes 4 to 7 and 11 to 14); thus, levels of acetylated  $\alpha$ -tubulin were higher than those in control mock-transduced or control

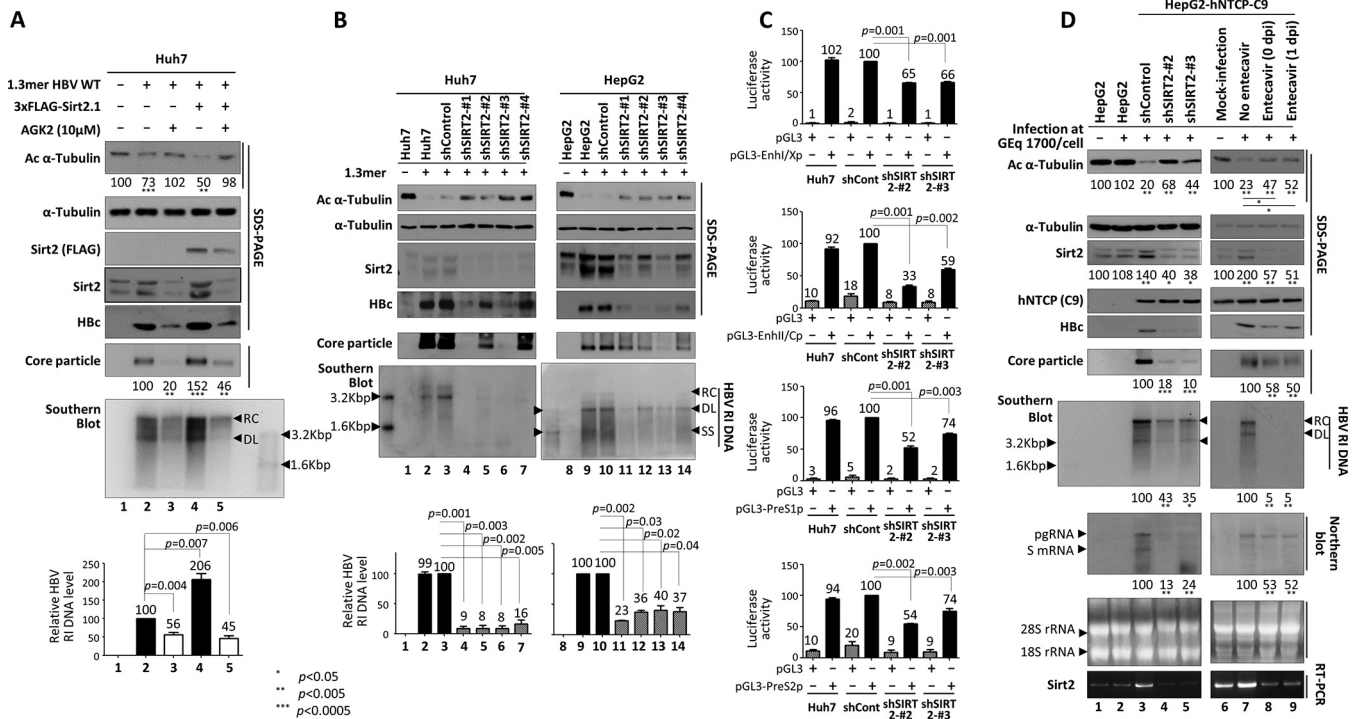


**FIG 4** Inhibition or knockdown of Sirt2 reduces HBV replication. (A) Treatment with AGK2, a potent Sirt2 inhibitor, reduces HBV replication. Huh7 cells were mock transfected (lane 1) or transfected with 4 μg of 1.3-mer HBV WT (ayw) (lanes 2 and 3) or with 4 μg of 1.3-mer HBV WT (ayw) plus 4 μg of the 3×FLAG-Sirt2.1 construct (lanes 4 and 5). Lanes 3 and 5 were treated for 72 h with AGK2 (10 μM) at the time of transfection. (B) HBV replication is decreased when Sirt2 is knocked down by shRNAs. Huh7 (lanes 1 to 7) and HepG2 (lanes 8 to 14) cells were transfected with lentivirus-like particles containing control shRNA (shControl) (lanes 3 and 10) or SIRT2-targeting shRNAs (shSIRT2-#1, shSIRT2-#2, shSIRT2-#3, and shSIRT2-#4) (lanes 4 to 7 and 11 to 14). The control (lanes 2 and 9) and transfected Huh7 (lanes 3 to 7) and HepG2 (lanes 10 to 14) cells were transiently transfected with 4 μg of 1.3-mer HBV WT (ayw) and lysed 72 h later. Lanes 1 and 8 are mock-transfected controls, which were adjusted with pcDNA3. (C) Promoter activities of Enhl/Xp, Enhl/Cp, PreS1p, and PreS2p are decreased upon Sirt2 knockdown. Freshly plated shControl-, shSIRT2-#2-, or shSIRT2-#3-transduced Huh7 cells were transfected with 2 μg of the indicated luciferase reporter vector containing null, Enhl/Xp, Enhl/Cp, PreS1p, or PreS2p regions. Lysates were prepared at 72 h posttransfection, and luciferase activity was measured. Luciferase activity relative to that in control shRNA-transduced cells is presented. Data are presented as the mean luciferase activities from four independent experiments. (D) Effects of Sirt2 knockdown or entecavir on HBV-infected cells. A total of 2 × 10<sup>5</sup> HepG2 (lane 2), HepG2-hNTCP-C9-shControl (lane 3), HepG2-hNTCP-C9-shSIRT2-#2 (lane 4), HepG2-hNTCP-C9-shSIRT2-#3 (lane 5), and HepG2-hNTCP-C9 (lanes 7 to 9) cells in 6-well plates were infected with 1.7 × 10<sup>3</sup> GEq per cell of HBV and lysed at 9 days postinfection (dpi). For Northern blotting (D, eighth panel), lysates were prepared at 5 days postinfection. Lane 1 (HepG2) and lane 6 (HepG2-hNTCP-C9) were mock infected. SDS-PAGE and Western blotting of proteins (A and D, first to fourth panels, and B, first to fourth panels), native agarose gel electrophoresis and Western blotting of core particles (A and D, sixth panels, and B, fifth panel), Southern blotting of HBV DNA (A and B, bottom panels, and D, seventh panel), and RT-PCR for Sirt2 mRNA (D, bottom panel) were performed as described in the legend of Fig. 1. Relative levels of acetylated α-tubulin, core particles, HBV RI DNA, and HBV mRNA were measured using ImageJ 1.46r. Data are presented as mean values from three independent experiments. Statistical significance was evaluated using Student's *t* test. *P* values relative to the respective control are shown.

shRNA-transduced Huh7 and HepG2 cells (Fig. 4B, top panel, lanes 2 and 3 versus 4 to 7 and lanes 9 and 10 versus 11 to 14). Upon Sirt2 knockdown, levels of HBV Hbc protein expression, core particle formation, and HBV DNA synthesis fell markedly (Fig. 4B).

Next, we examined the effect of Sirt2 knockdown on HBV enhancer and promoter activities using a luciferase reporter assay. Mock-, control shRNA-, shSIRT2-#2-, or shSIRT2-#3-transduced Huh7 cells were transfected with pGL3 empty or pGL3-Enhl/Xp (Fig. 4C, top panel), pGL3 empty or pGL3-Enhl/Cp (Fig. 4C, second panel), pGL3 empty or pGL3-PreS1p (Fig. 4C, third panel), and pGL3 empty or pGL3-PreS2p (Fig. 4C, bottom panel). The HBV enhancer and promoter (Enhl/Xp, Enhl/Cp, preS1p, and preS2p, respectively) activities in Sirt2 knockdown cells were lower than those in mock- and control shRNA-transduced Huh7 cells (Fig. 4C).

To validate the Sirt2 effect on HBV replication, we employed an HBV infection experiment using HepG2-hNTCP cells, which are susceptible to HBV infection. Following infection of HepG2-hNTCP-C9 cells that had been transfected with lentiviral control shRNA or Sirt2 shRNAs (shSIRT2-#2 or -#3), we detected markedly reduced HBV pgRNA and subgenomic RNA levels, Hbc protein expression, core particle formation, and HBV DNA synthesis in Sirt2 knockdown cells compared to control shRNA-transduced cells

(Fig. 4D, fifth to eighth panels, lane 3 versus 4 and 5). Sirt2 knockdown cells showed reduced Sirt2 RNA and protein expression (Fig. 4D, 3rd and 10th panels, lane 3 versus 4 and 5); thus, the levels of acetylated  $\alpha$ -tubulin were higher than those in control shRNA-transduced HepG2-hNTCP-C9 cells (Fig. 4D, top panel, lane 3 versus 4 and 5). Since HepG2 cells are not susceptible to HBV infection, mock-infected and HBV-infected HepG2 cells showed comparable Sirt2 expression (Fig. 4D, third panel, lanes 1 and 2) and acetylated  $\alpha$ -tubulin (Fig. 4D, top panel, lanes 1 and 2) levels.

In order to examine the effect of entecavir on Sirt2 in the infection system, HBV-infected HepG2-hNTCP-C9 cells were treated with entecavir (1  $\mu$ M) at the time of infection (Fig. 4D, lane 8) or 1 day after infection (lane 9). As expected, the endogenous Sirt2 level was higher in HBV-infected HepG2-hNTCP-C9 cells than in mock-infected control HepG2-hNTCP-C9 cells (Fig. 4D, third panel, lane 6 versus 7). Also, the endogenous Sirt2 level was markedly reduced in entecavir-treated HBV-infected HepG2-hNTCP-C9 cells (Fig. 4D, third panel, lane 6 versus 8 and 9). Accordingly, the Sirt2 mRNA level fell significantly upon entecavir treatment (Fig. 4D, bottom panel, lane 6 versus 8 and 9). Since entecavir-treated HepG2-hNTCP-C9 cells showed reduced Sirt2 expression, acetylated  $\alpha$ -tubulin levels were higher in entecavir-treated, HBV-infected cells than in HBV-infected cells (Fig. 4D, top panel, lane 7 versus 8 and 9).

#### **Overexpression of a Sirt2 dominant negative mutant impairs HBV replication.**

Since HBV replication was impaired by Sirt2 inhibition or knockdown (Fig. 4), we next investigated whether Sirt2 activity affects the HBV life cycle. A Sirt2 dominant negative (DN) mutant was constructed by exchanging the catalytically active histidine 187 (CAC) in Sirt2 for tyrosine (TAC), thereby inactivating Sirt2 deacetylase activity (41). Upon expression of the inactive Sirt2 DN mutant, acetylated  $\alpha$ -tubulin levels increased (Fig. 5A, top panel, lanes 4 and 8). Levels of Hbc protein expression, HBV core particle formation, and HBV DNA replication in Sirt2 DN mutant-expressing cells were lower than those in Huh7 and HepG2 cells transfected with the 1.3-mer HBV WT (Fig. 5A, lane 2 versus 4 and lane 6 versus 8).

**Expression of replication-deficient mutant HBV impairs Sirt2 activity.** Since Sirt2 expression and  $\alpha$ -tubulin deacetylation were increased in HBV WT-replicating cells (Fig. 1A, lanes 2, 4, and 6, and B and C, lanes 2) but fell in replication-deficient HBV mutant-transfected and RT inhibitor-treated cells (Fig. 1B and C, lanes 3 and 4), we compared the effects of Sirt2 WT and the Sirt2 DN mutant on HBV WT-replicating and replication-deficient mutant-expressing Huh7 cells. As expected, Sirt2 WT- or Sirt2 DN mutant-transfected Huh7 cells showed elevated  $\alpha$ -tubulin deacetylation or elevated  $\alpha$ -tubulin acetylation, respectively (Fig. 5B, top panel, lane 3 versus 4). Consistent with the data in Fig. 5A, HBV WT- and Sirt2 WT-cotransfected cells showed higher levels of  $\alpha$ -tubulin deacetylation and HBV replication than HBV WT-transfected cells (Fig. 5B, top and bottom panels, lane 5 versus 6), and HBV WT- and Sirt2 DN-cotransfected cells showed lower levels of  $\alpha$ -tubulin deacetylation and HBV replication than HBV WT-transfected cells (lane 5 versus 7). Surprisingly, replication-deficient HBV-expressing cells showed a greater elevation of  $\alpha$ -tubulin acetylation, although Sirt2 WT was overexpressed (Fig. 5B, top panel, lanes 9 and 12), as did Sirt2 DN mutant-overexpressing cells (lanes 10 and 13), indicating that replication-deficient mutant HBV impairs Sirt2 activity.

**Increased expression of Sirt2 in HBV-replicating cells activates the AKT/GSK-3 $\beta$ / $\beta$ -catenin signaling pathway through the AKT/Sirt2 interaction.** Sirt2 is a novel AKT binding partner and is required for full activation of AKT (16, 25). Also, Sirt2 is upregulated in HCC cells and mediates the epithelial-to-mesenchymal transition through the AKT/GSK-3 $\beta$ / $\beta$ -catenin signaling cascade (16). Since endogenous Sirt2 was upregulated in HBV WT-replicating cells but downregulated in replication-deficient mutant HBV-expressing cells (Fig. 1), we investigated whether Sirt2-mediated activation of the AKT/GSK-3 $\beta$ / $\beta$ -catenin signaling pathway may be involved in HBV replication in Huh7 and HepG2 cells. HBV WT-transfected Huh7 or HepG2 cells showed activation of AKT (i.e., phosphorylation of T308 and S473) (Fig. 6A, fifth and sixth panels, lane 1 versus 2 and lane 4 versus 5). GSK-3 $\beta$  activity was inhibited, as shown by phosphory-

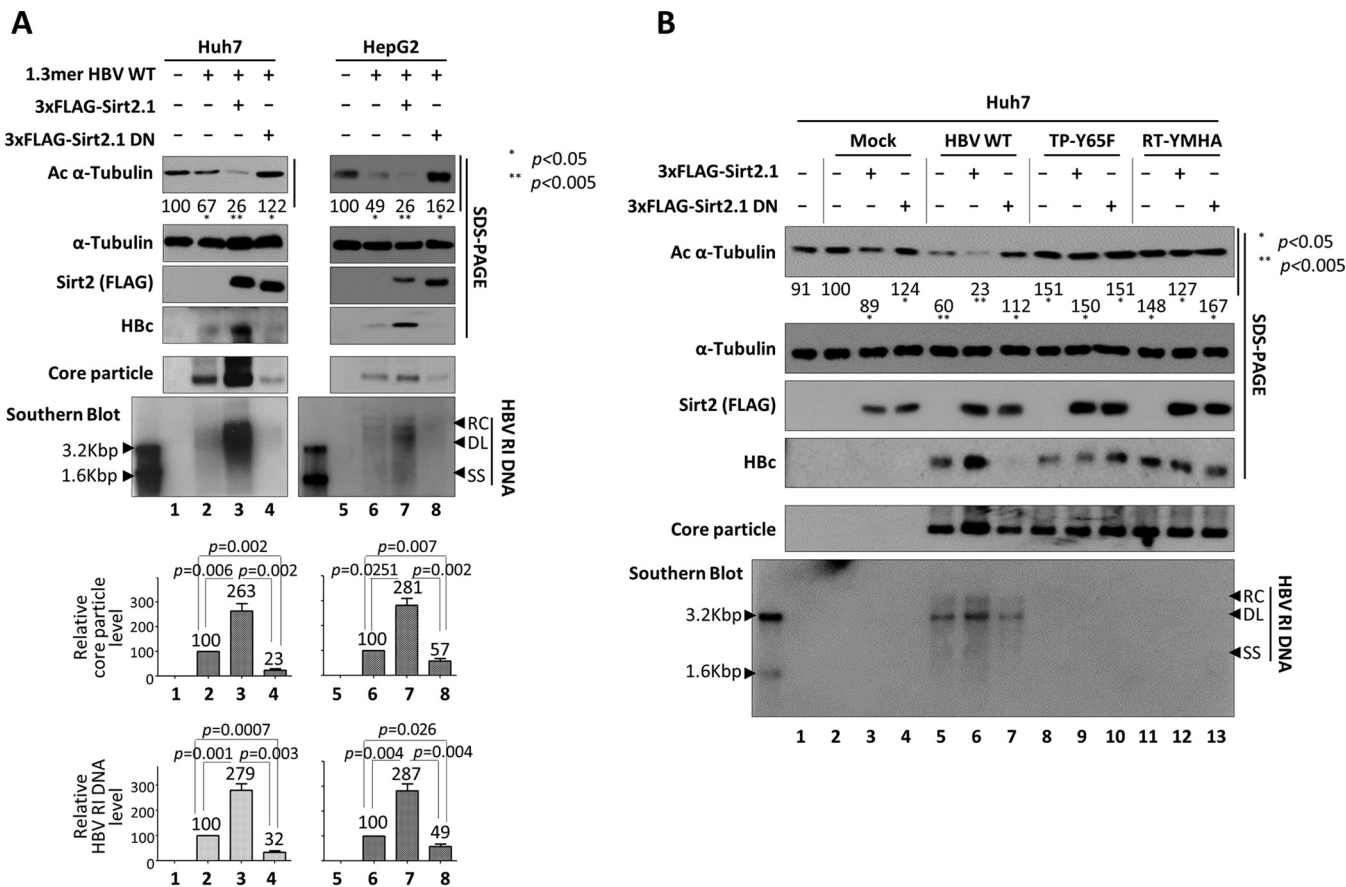


**FIG 5** Replication of HBV WT is inhibited by overexpression of a Sirt2.1 dominant negative (DN) mutant, and HBV replication-deficient mutant expression impairs Sirt2 activity. (A) A Sirt2 DN mutant inhibits HBV replication. Huh7 (lanes 1 to 4) or HepG2 (lanes 5 to 8) cells were mock transfected (lanes 1 and 5), transfected with 4  $\mu$ g of 1.3-mer HBV WT (ayw) (lanes 2 and 6), or cotransfected with 4  $\mu$ g of 3 $\times$ FLAG-Sirt2.1 WT (lanes 3 and 7) or the 3 $\times$ FLAG-Sirt2.1 DN mutant (lanes 4 and 8) along with 4  $\mu$ g of 1.3-mer HBV WT (ayw). (B) In HBV replication-deficient mutant-expressing cells, Sirt2 activity is impaired, with no deacetylation of  $\alpha$ -tubulin (as in Sirt2 DN-expressing cells). Huh7 cells were mock transfected (lane 1) or transiently cotransfected with 4  $\mu$ g of 3 $\times$ FLAG-Sirt2.1 WT (lanes 3, 6, 9, and 12) or 4  $\mu$ g of 3 $\times$ FLAG-Sirt2.1 DN (lanes 4, 7, 10, and 13) along with mock (lanes 2 to 4), HBV WT (lanes 5 to 7), or replication-incompetent TP-Y65F (lanes 8 to 10) or RT-YMHA (lanes 11 to 13) mutants. Lysates were prepared at 72 h posttransfection. The amount of transfected DNA was adjusted using pcDNA3. SDS-PAGE and Western blotting of proteins (first to fourth panels), native agarose gel electrophoresis and Western blotting of core particles (fifth panel), and Southern blotting of HBV DNA (bottom panel) were performed as described in the legend of Fig. 1. Relative levels of acetylated  $\alpha$ -tubulin, core particles, and HBV RI DNA were measured by ImageJ 1.46r. Data are presented as mean values from three independent experiments. Statistical significance was evaluated using Student's *t* test. *P* values relative to the respective controls are shown.

lation at S9 (Fig. 6A, eighth panel, lane 1 versus 2 and lane 4 versus 5). Subsequently,  $\beta$ -catenin levels increased (Fig. 6A, 11th panel, lane 1 versus 2 and lane 4 versus 5). Cotransfection of Sirt2 and the 1.3-mer HBV WT increased AKT activation even further (Fig. 6A, 5th and 6th panels, lane 2 versus 3 and lane 5 versus 6), GSK-3 $\beta$  activity was further inhibited (Fig. 6A, 9th panel, lane 2 versus 3 and lane 5 versus 6), and  $\beta$ -catenin levels increased further (Fig. 6A, 11th panel, lane 2 versus 3 and lane 5 versus 6). This indicates that Sirt2 upregulates HBV replication via the AKT/GSK-3 $\beta$ / $\beta$ -catenin signaling pathway.

Since Sirt2 interacts with AKT (16, 25), we next examined the interaction between Sirt2 and AKT in HBV-replicating cells. When HBV was replicating, the Sirt2-AKT interaction increased (Fig. 6B, lane 6), indicating that upregulation of Sirt2 in HBV-replicating cells activates AKT more strongly through the enhanced Sirt2-AKT interaction; this leads to greater inactivation of GSK-3 $\beta$  and increased  $\beta$ -catenin levels in HBV-replicating cells.

**Sirt2-mediated upregulation of HBV replication is independent of HBx.** Since HBx upregulates Sirt2 (18), activates AKT (29, 46), and is essential for Wnt/ $\beta$ -catenin signaling in hepatoma cells (47–49), it is possible that increased Sirt2 and AKT/GSK-3 $\beta$ / $\beta$ -catenin signaling in HBV-replicating cells is caused by overexpression of HBx.

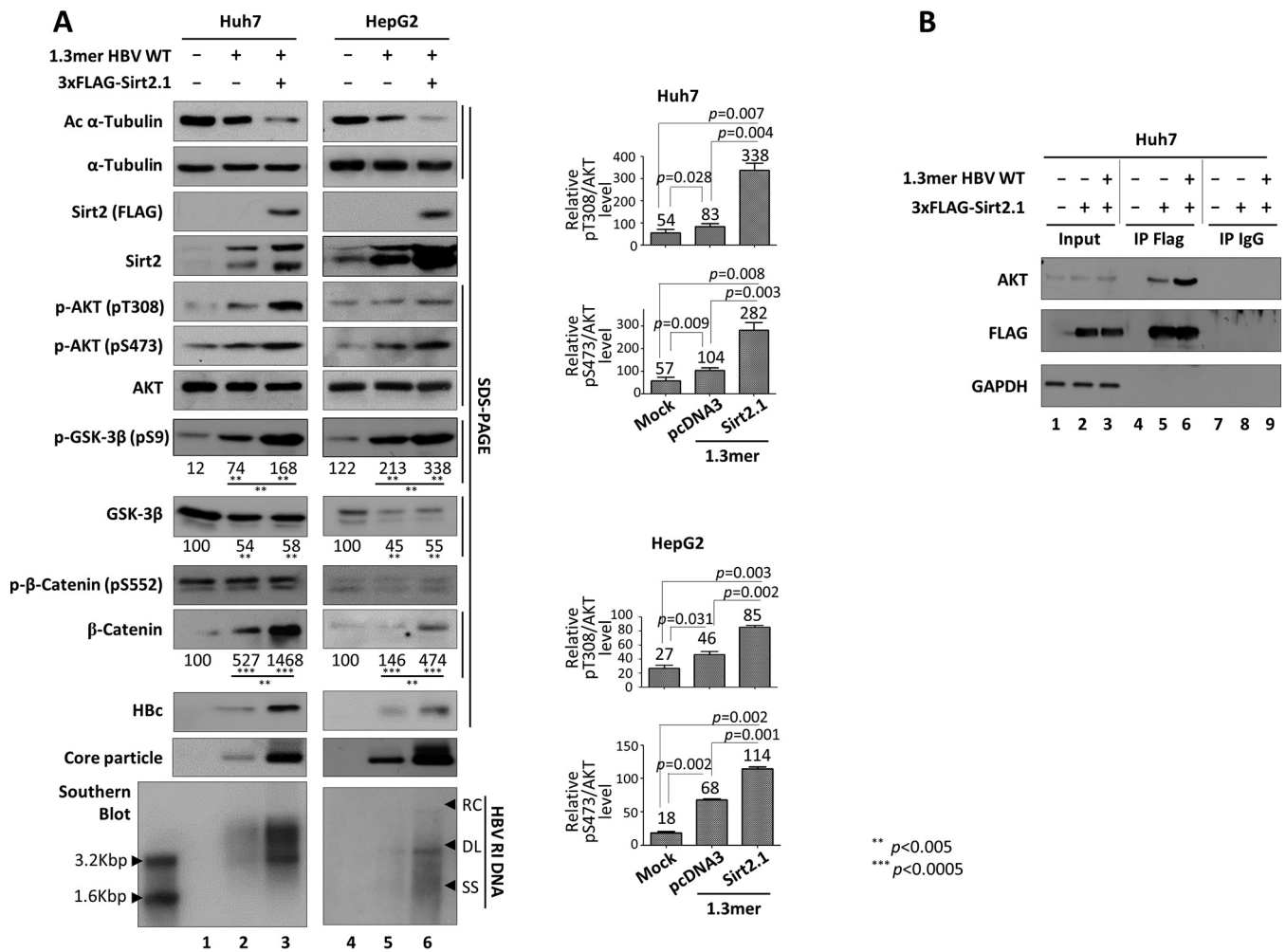


**FIG 6** HBV replication increases Sirt2-mediated AKT/GSK-3β/β-catenin signaling via AKT/Sirt2 interaction. (A) HBV replication increases Sirt2-mediated AKT/GSK-3β/β-catenin signaling. Huh7 (lanes 1 to 3) or HepG2 (lanes 4 to 6) cells were mock transfected (lanes 1 and 4), transfected with 4 μg of 1.3-mer HBV WT (ayw) (lanes 2 and 5), or cotransfected with 4 μg of 1.3-mer HBV WT (ayw) plus 4 μg of 3×FLAG-Sirt2.1 (lanes 3 and 6). The amount of transfected DNA was adjusted using pcDNA3 (lanes 2 and 5). Lysates were prepared at 72 h posttransfection. SDS-PAGE and Western blotting for core particles (13th panel), native agarose gel electrophoresis and Western blotting for core particles (13th panel), and Southern blotting of HBV DNA (bottom panel) were performed as described in the legend of Fig. 1. Relative levels of total and active AKT (pT308 and pS473), total/phosphorylated (S552) β-catenin, and total/phosphorylated (S9) GSK-3β were measured using ImageJ 1.46r. Data are presented as mean values from three independent experiments. Statistical significance was evaluated using Student's *t* test. *P* values relative to the respective controls are shown. (B) HBV replication increases the AKT/Sirt2 interaction. Huh7 cells were mock transfected (lane 1) or transfected with 4 μg of the 3×FLAG-Sirt2.1 construct (lane 2) or 4 μg of 1.3-mer HBV WT (ayw) plus 4 μg of the 3×FLAG-Sirt2.1 construct (lane 3). At 3 days posttransfection, cell lysates were immunoprecipitated (IP) with mouse monoclonal anti-FLAG M2 (catalog number F1804; Sigma) and then immunoblotted with rabbit polyclonal anti-AKT (catalog number 9272S; Cell Signaling Technology). Mouse normal IgG was used as a negative control (catalog number 12-371; Merck Millipore). Immunoprecipitated proteins were subjected to SDS-PAGE and immunoblotting with anti-AKT, anti-FLAG, and anti-GAPDH antibodies.

Therefore, we asked whether Sirt2-mediated upregulation of HBV replication is HBx dependent. HepG2 cells were transiently transfected with the 1.3-mer HBV WT or with an HBx-deficient mutant in the presence or absence of 3×FLAG-tagged Sirt2.1 (Fig. 7A). The level of HBV replication in HBx-deficient mutant-transfected cells was lower than that in HBV WT-transfected cells (50–52) (Fig. 7A, 11th to 13th panels, lane 2 versus 4). Upon reduced HBV replication in HBx-deficient mutant-transfected cells, increased endogenous Sirt2, AKT activation (phosphorylation at T308 and S473), GSK-3β inhibition (inhibitory phosphorylation at S9), and increased β-catenin expression were lower than those in HBV WT-transfected cells (Fig. 7A, 4th to 6th, 8th, and 10th panels, lane 2 versus 4); however, the levels of endogenous Sirt2, AKT activation, GSK-3β inhibition, and increased β-catenin expression were higher than those in mock-transfected cells (lane 1 versus 4). Also, α-tubulin was acetylated to a greater extent in HBx-deficient

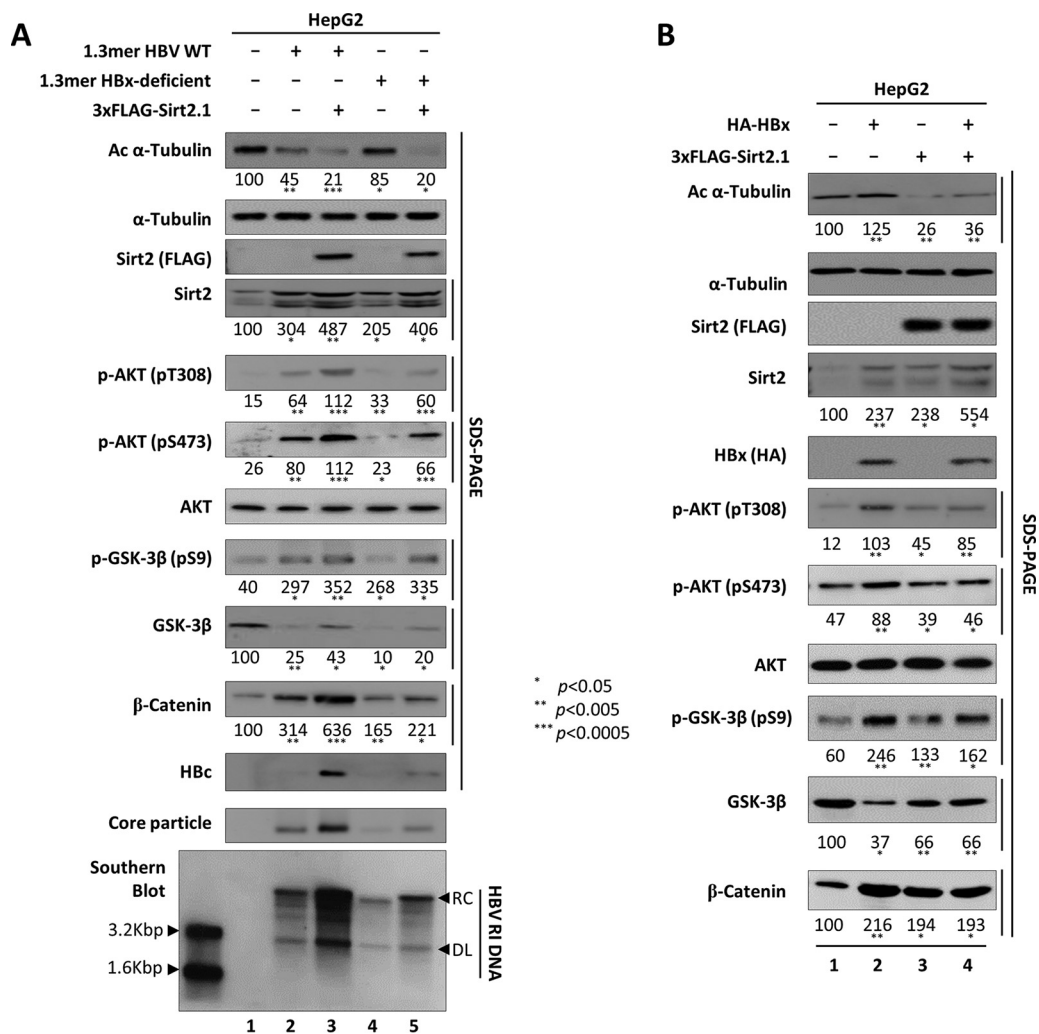


**FIG 7** Sirt2-mediated upregulation of HBV replication is independent of HBx. (A) Overexpression of Sirt2 increases replication of a HBx-deficient mutant via AKT/GSK-3 $\beta$ / $\beta$ -catenin signaling. HepG2 cells were mock transfected (lane 1) or transfected with 4  $\mu$ g of 1.3-mer HBV WT (ayw) (lanes 2 and 3) or with 4  $\mu$ g of the 1.3-mer HBx-deficient (ayw) mutant (lanes 4 and 5) in the absence (lanes 2 and 4) or presence (lanes 3 and 5) of the 3 $\times$ FLAG-Sirt2.1 (4  $\mu$ g) construct. Lysates were prepared at 72 h posttransfection. The amount of transfected DNA was adjusted using pcDNA3 (lanes 2 and 4). SDS-PAGE and Western blotting of proteins (1st to 11th panels), native agarose gel electrophoresis and Western blotting for core particles (12th panel), and Southern blotting of HBV DNA (bottom panel) were performed as described in the legend of Fig. 1. (B) Activation of the AKT/GSK-3 $\beta$ / $\beta$ -catenin signaling pathway by HBx and Sirt2 is not synergistic. HepG2 cells were transfected with 4  $\mu$ g of HA-HBx (lane 2), 4  $\mu$ g of the 3 $\times$ FLAG-Sirt2.1 construct (lane 3), or 4  $\mu$ g of HA-HBx plus 4  $\mu$ g of the 3 $\times$ FLAG-Sirt2.1 construct (lane 4). Lysates were prepared at 72 h posttransfection. The amount of transfected DNA was adjusted using pcDNA3 (lanes 2 and 3). SDS-PAGE and Western blotting of protein (1st to 11th panels) were performed as described in the legend of Fig. 1. Relative levels of total and active AKT (pT308 and pS473), total/phosphorylated (S9) GSK-3 $\beta$ , and  $\beta$ -catenin were measured using ImageJ 1.46r. Data are presented as mean values from three independent experiments. Statistical significance was evaluated using Student's *t* test. *P* values relative to the respective controls are shown.

mutant-transfected cells (Fig. 7A, top panel, lane 4). HBV replication was upregulated upon cotransfection of the HBx-deficient mutant and 3 $\times$ FLAG-tagged Sirt2.1 constructs (Fig. 7A, 11th to 13th panels, lane 4 versus 5). Also, AKT was activated, GSK-3 $\beta$  was inhibited, and  $\beta$ -catenin levels increased to a greater extent than in HBx-deficient mutant-transfected cells (Fig. 7A, 5th to 10th panels, lane 4 versus 5). Therefore, Sirt2-mediated AKT/GSK-3 $\beta$ / $\beta$ -catenin signaling and upregulated HBV replication were independent of HBx (Fig. 7A, 11th to 13th panels, lane 4 versus 5).

To examine whether HBx and the Sirt2-mediated AKT/GSK-3 $\beta$ / $\beta$ -catenin signaling pathway show synergistic effects, HepG2 cells were transiently (co)transfected with hemagglutinin (HA)-HBx, 3 $\times$ FLAG-tagged Sirt2.1, or HA-HBx and 3 $\times$ FLAG-tagged

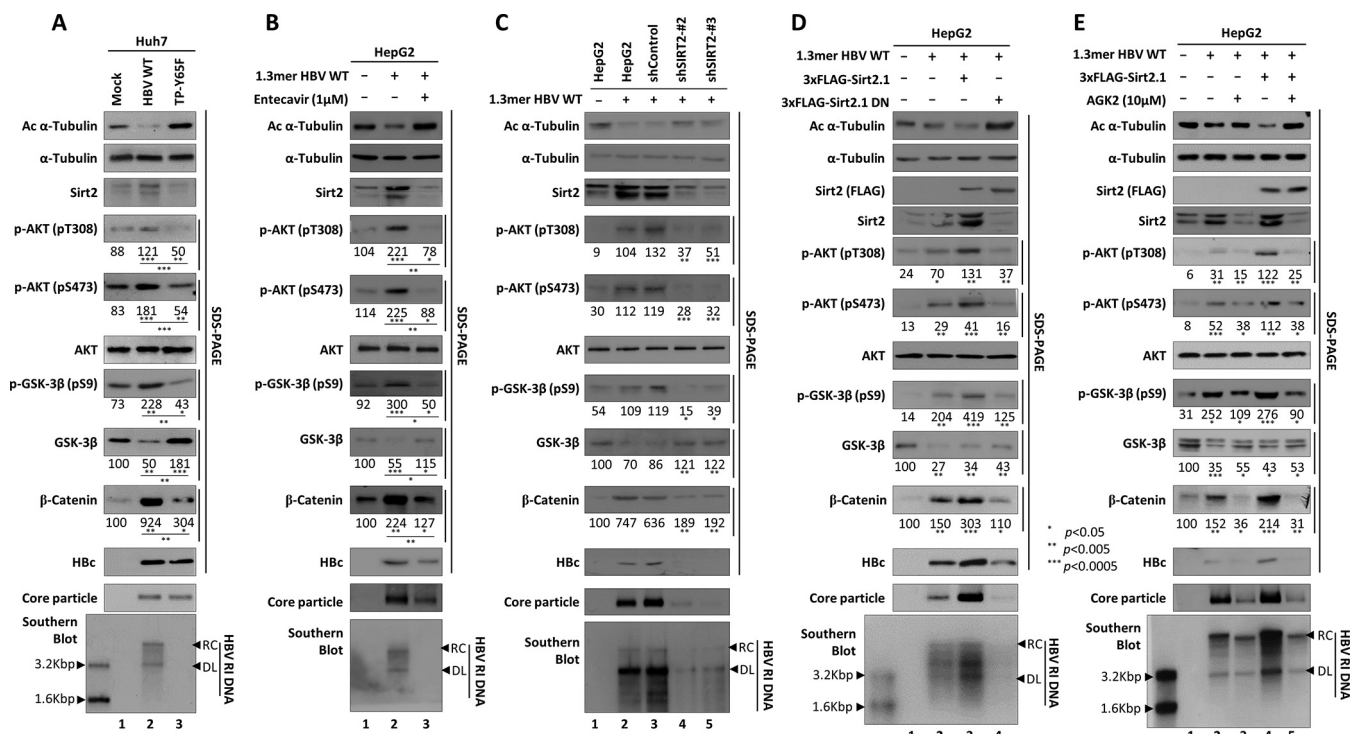


**FIG 8** AKT/GSK-3 $\beta$ / $\beta$ -catenin signaling is downregulated in HBV replication-deficient mutant-transfected cells. (A) AKT/GSK-3 $\beta$ / $\beta$ -catenin signaling is downregulated in HBV replication-deficient mutant-transfected cells. Huh7 cells were transfected with 4  $\mu$ g of HBV WT (lane 2) or the TP-Y65F mutant (lane 3). (B) AKT/GSK-3 $\beta$ / $\beta$ -catenin signaling is downregulated in entecavir-treated 1.3-mer HBV WT-transfected HepG2 cells. HepG2 cells were mock transfected (lane 1) or transfected with 4  $\mu$ g of 1.3-mer HBV WT (lanes 2 and 3). Lane 3 was treated with entecavir (1  $\mu$ M) at 24 h posttransfection for 48 h. (C) Knockdown of Sirt2 by shRNAs downregulates AKT/GSK-3 $\beta$ / $\beta$ -catenin signaling. HepG2 cells were transfected with lentivirus-like particles containing control shRNA (shControl) (lane 3) or SIRT2-targeting shRNAs (shSIRT2-#2 and shSIRT2-#3) (lanes 4 and 5). Mock-transduced control (lane 2) and shRNA-transduced HepG2 (lanes 3 to 5) cells were transiently transfected with 4  $\mu$ g of 1.3-mer HBV WT (ayw). Lane 1 is the mock-transfected control. (D) Expression of a Sirt2 DN mutant downregulates AKT/GSK-3 $\beta$ / $\beta$ -catenin signaling. HepG2 cells were mock transfected (lane 1) or cotransfected with 4  $\mu$ g of 1.3-mer HBV WT (ayw) (lanes 2 to 4) plus 4  $\mu$ g of pcDNA3 (lane 2) or 3 $\times$ FLAG-Sirt2.1 (lane 3) or the 3 $\times$ FLAG-Sirt2.1 DN mutant (lane 4). (E) Treatment with AGK2 downregulates AKT/GSK-3 $\beta$ / $\beta$ -catenin signaling. HepG2 cells were cotransfected with 4  $\mu$ g of 1.3-mer HBV WT (ayw) (lanes 2 to 5) plus 4  $\mu$ g of pcDNA3 (lanes 2 and 3) or 3 $\times$ FLAG-Sirt2.1 (lanes 4 and 5). Lanes 3 and 5 were treated with AGK2 (10  $\mu$ M) at the time of transfection (treatment lasted 72 h). Lysates were prepared at 72 h posttransfection. SDS-PAGE and Western blotting of proteins (A to C, 1st to 10th panels; D and E, 1st to 11th panels), native agarose gel electrophoresis and Western blotting of core particles (A to C, 11th panels; D and E, 12th panels), and Southern blotting of HBV DNA (bottom panels) were performed as described in the legend of Fig. 1. Relative levels of total and active AKT (pT308 and pS473), total/phosphorylated (S552)  $\beta$ -catenin, and total/phosphorylated (S9) GSK-3 $\beta$  were measured by ImageJ 1.46r. Data are presented as mean values from three independent experiments. Statistical significance was evaluated using Student's *t* test. *P* values relative to the respective controls are shown.

Sirt2.1 (Fig. 7B). Upon overexpression of HBx, AKT/GSK-3 $\beta$ / $\beta$ -catenin signaling was more active than in 3 $\times$ FLAG-tagged Sirt2.1-transfected or 3 $\times$ FLAG-tagged Sirt2.1/HBx-cotransfected cells, suggesting a lack of synergism (Fig. 7B, 6th, 7th, 9th, and 10th panels, lane 2 versus 3 and 4). Even though HBx upregulates Sirt2 (Fig. 7B, fourth panel, lane 2 versus 1) (18) and activates AKT/GSK-3 $\beta$ / $\beta$ -catenin signaling,  $\alpha$ -tubulin was more acetylated in HBx-overexpressing cells (Fig. 7B, top panel, lane 2 versus 1, 3, and 4), indicating that HBx-mediated AKT/GSK-3 $\beta$ / $\beta$ -catenin signaling is different from Sirt2-mediated AKT/GSK-3 $\beta$ / $\beta$ -catenin signaling. Also, the elevation of the HBx-mediated Sirt2 level (18) may not be involved in Sirt2 enzymatic activity, as shown by tubulin deacetylation.

**AKT/GSK-3 $\beta$ / $\beta$ -catenin signaling is downregulated in HBV replication-deficient mutant-transfected, entecavir-treated, Sirt2 DN mutant-overexpressing, and Sirt2-inhibited cells.** As shown in Fig. 6A, when HBV is replicating, Sirt2 is upregulated, and AKT/GSK-3 $\beta$ / $\beta$ -catenin is activated. Therefore, we wanted to examine AKT/GSK-3 $\beta$ / $\beta$ -catenin signaling in replication-deficient, HBV TP-Y65F mutant-transfected cells. Huh7 cells were transiently transfected with HBV WT or a TP-Y65F mutant (Fig. 8A). Expression of the replication-deficient mutant did not increase AKT activation, GSK-3 $\beta$  inhibition, and  $\beta$ -catenin levels (unlike in HBV WT-transfected cells) (Fig. 8A, fourth to

ninth panels, lane 2 versus 3); however,  $\beta$ -catenin levels were higher than those in mock-transfected cells (ninth panel, lane 1 versus 3). These results indicate that HBV replication upregulates Sirt2 and that upregulated Sirt2 mediates AKT/GSK-3 $\beta$ / $\beta$ -catenin signaling, whereas replication-deficient mutant expression downregulates Sirt2-AKT/GSK-3 $\beta$ / $\beta$ -catenin signaling. Similarly, when we treated 1.3-mer HBV WT-transfected HepG2 cells with entecavir (1  $\mu$ M), Sirt2-mediated AKT/GSK-3 $\beta$ / $\beta$ -catenin signaling was downregulated as in replication-deficient mutant-transfected cells (Fig. 8B). Of note, very low (undetectable) expression levels of HBx in replication-deficient mutant-transfected or entecavir-treated cells may stabilize  $\beta$ -catenin (Fig. 8A and B, ninth panels, lanes 3).

To further confirm that the knockdown of Sirt2 decreases AKT/GSK-3 $\beta$ / $\beta$ -catenin signaling and downregulates HBV replication (Fig. 4C), we examined AKT/GSK-3 $\beta$ / $\beta$ -catenin signaling in Sirt2 knockdown cells. As expected, Sirt2 knockdown failed to stimulate AKT/GSK-3 $\beta$ / $\beta$ -catenin signaling and reduced HBV replication (Fig. 8C, lanes 2 and 3 versus 4 and 5).

To further confirm that overexpression of active Sirt2 further increases AKT/GSK-3 $\beta$ / $\beta$ -catenin signaling and upregulates HBV replication (Fig. 6A, lanes 3 and 6), we examined the effects of overexpression of a Sirt2 DN mutant on the AKT/GSK-3 $\beta$ / $\beta$ -catenin signaling pathway. Since overexpression of Sirt2 DN reduced HBV replication (Fig. 5 and 8D, lane 4), we expected that the AKT/GSK-3 $\beta$ / $\beta$ -catenin signaling pathway would not be activated. As expected, AKT activation decreased, GSK-3 $\beta$  was activated, and  $\beta$ -catenin levels decreased in the presence of inactive Sirt2 (Fig. 8D, lanes 2 and 3 versus 4).

Since catalytically active Sirt2 mediates AKT/GSK-3 $\beta$ / $\beta$ -catenin signaling and upregulates HBV replication (Fig. 8D), we further examined AKT/GSK-3 $\beta$ / $\beta$ -catenin signaling in the presence of the potent Sirt2 inhibitor AGK2 (10  $\mu$ M) (45) (Fig. 8E). Since AGK2 inhibited HBV replication (Fig. 4A and 8E, lanes 3 and 5), we expected that it would inactivate AKT/GSK-3 $\beta$ / $\beta$ -catenin signaling. As expected, upon inhibition of Sirt2, the AKT/GSK-3 $\beta$ / $\beta$ -catenin signaling pathway was also inhibited (Fig. 8E, lanes 3 and 5). Taken together, the results demonstrate that HBV replication upregulates Sirt2, which activates the AKT/GSK-3 $\beta$ / $\beta$ -catenin signaling pathway through a physical interaction with AKT. In addition, inhibiting Sirt2 reduces HBV replication by inactivating the AKT/GSK-3 $\beta$ / $\beta$ -catenin signaling pathway.

## DISCUSSION

HCC is one of the most common malignant cancers and the third most frequent cause of cancer-related death worldwide (53). Indeed, approximately 750,000 new HCC cases are reported each year (54). Highly aggressive HCC is likely to be metastatic because HCC cells migrate through the extracellular matrix (ECM) and vascular wall and invade the circulation, whereupon they can promote angiogenesis (55). Among the several proteins and pathways that promote HCC metastasis, Sirt2 mediates epithelial mesenchymal transition (EMT) and helps HCC cells to metastasize by modulating the AKT/GSK-3 $\beta$ / $\beta$ -catenin signaling pathway (16). In addition, high levels of Sirt2 are associated with a more advanced tumor stage (16) and reduced patient survival (16, 56). Many HCC cases are linked to chronic HBV infection, and high levels of HBV replication are linked to HCC development (57–59). In accordance with these notions, we found that the expression of endogenous Sirt2 was increased in HBV-replicating cells (Fig. 1; 4A, B, and D; 6A; 7; and 8), which in turn activated AKT, downregulated GSK-3 $\beta$ , and increased the stability of  $\beta$ -catenin (Fig. 6A and 8). However, in replication-deficient HBV TP-Y65F or RT-YMHA mutant-expressing cells or 1.3-mer HBV WT-transfected RT inhibitor-treated HepG2 cells, endogenous Sirt2 levels fell, along with tubulin deacetylation (Fig. 1B and C and 8A and B), even though undetectable levels of HBx were present in these cells.

To our dismay, Cheng et al. (18) also reported that Sirt2 and HBV replication are linked, while we were preparing the manuscript. However, they did not investigate Sirt2-mediated AKT/GSK-3 $\beta$ / $\beta$ -catenin signaling on HBV-replicating and replication-

deficient mutant-expressing cells and HBx dependency. Consistent with their report, we also found that HBx upregulates endogenous Sirt2 levels (Fig. 7B) (18); however, Sirt2 deacetylase activity was not activated by HBx, and downstream signaling was not dependent on HBx (Fig. 7B). We also showed that Sirt2-mediated enhancement of HBV DNA synthesis does not depend on HBx (Fig. 7A). Even though HBx upregulates endogenous Sirt2 (18), activates AKT (29, 46), and upregulates Wnt/ $\beta$ -catenin signaling via pERK (47) and c-Src (48, 60), but independently of GSK-3 $\beta$  (49), we demonstrated that Sirt2-mediated AKT/GSK-3 $\beta$ / $\beta$ -catenin signaling (16) was independent of HBx (Fig. 7). We postulated that Sirt2- and HBx-mediated signaling may exert synergistic effects; however, none were detected (Fig. 7B), further strengthening the argument that HBx or Sirt2 activates AKT and  $\beta$ -catenin signaling independently, although both may converge to cause hepatocarcinogenesis. Unlike Sirt2, Sirt1 binds to HBx and shows synergy and mutual dependence in terms of activating HBV transcription (61); also, HBx sequesters Sirt1 to weaken the inhibitory interaction between Sirt1 and  $\beta$ -catenin, leading to increased expression of the  $\beta$ -catenin protein (62).

Sirts (Sirt1 to -7) are broad-spectrum, evolutionarily conserved viral restriction factors (63). Here, we demonstrate that Sirt2.1 increases HBV transcription (Fig. 3) and DNA replication (Fig. 2C). However, the effects of Sirt2.2, Sirt2.5, and Sirt4 to -7 on HBV replication need to be determined in future studies.

Although it is hypothesized that acetylated and/or deetyrosinated tubulins are a hallmark of stabilized microtubules, a recent idea suggests that posttranslational tubulin modifications, such as acetylation, affect microtubule dynamics (64). Hence, tubulin acetylation may play an important role in regulating microtubule function; however, the underlying mechanism(s) is not clear (65, 66). Viruses have adopted multiple strategies to hijack cellular processes to support their own propagation. Several reports demonstrate the roles of acetylated microtubules in virus infection. For example, human herpesvirus 8 induces the acetylation of microtubules to deliver its DNA to the nucleus (67); adenovirus induces microtubule acetylation to facilitate viral entry (68); influenza A virus increases the acetylation of  $\alpha$ -tubulin to facilitate the transport of viral components (69); human immunodeficiency virus type 1 (HIV-1) induces microtubule acetylation to promote infection, and HDAC6 overexpression or depletion inhibits or increases HIV-1 infection, respectively (70, 71); and finally, acetylated  $\alpha$ -tubulin increases the replication of human parainfluenza virus type 3 by regulating inclusion body fusion (72). However, the effects of acetylation and deacetylation on microtubule dynamics during virus infection remain elusive. Here, we demonstrated that when HBV is replicating,  $\alpha$ -tubulin is deacetylated through upregulated endogenous Sirt2 (Fig. 1A and 8A); therefore, acetylation and microtubule dynamics during HBV infection may need to be explored in the future.

When we inhibited Sirt2 using AGK2, a Sirt2 DN mutant, or Sirt2 shRNAs, we found that HBV replication was inhibited markedly. Hence, Sirt2 may be a molecular target for controlling HBV replication, and Sirt2 inhibition may be a novel therapeutic strategy for treating chronic HBV infection, liver fibrosis, cirrhosis, and HCC; it may also prevent HCC development.

## MATERIALS AND METHODS

**Vector construction.** A HBV WT plasmid from subtype adwR9 was used, in which transcription of pgRNA is controlled by the CMV IE promoter (37). Also, HBV replication-deficient TP-Y65F (priming reaction-deficient) and RT-YMHA (RT reaction-deficient) mutants (37) were used. Subtype ayw, a replication-competent 1.3-mer from HBV WT, and HBx-deficient mutant plasmids were kind gifts from W. S. Ryu (Yonsei University, South Korea). The human NTCP-C9 (hNTCP-C9) construct in pcDNA6.1 was a kind gift from W. Li (2). From this construct, pCDH-hNTCP-C9 was generated using the primers listed in Table 1. The green fluorescent protein (GFP)-tagged Sirt2.1 and Myc-tagged HDAC6 plasmids were kindly provided by K. W. Lee (Chonnam National University, South Korea) (73). The 3 $\times$ FLAG-tagged Sirt2.1 construct was generated from GFP-tagged Sirt2.1 using the primers listed in Table 1. The 3 $\times$ FLAG-tagged Sirt2.2 and Sirt2.5 constructs were generated from the 3 $\times$ FLAG-tagged Sirt2.1 construct using the primers listed in Table 1. To construct a DN mutant of Sirt2.1, the codon encoding the catalytic histidine (CAC) at position 187 was mutated to tyrosine (TAC) by PCR-based site-directed mutagenesis using mutagenic primers (Table 1). To generate short hairpin RNA (shRNA)-containing constructs targeting the SIRT2 gene, four optimal 21-mer RNAs were selected from human SIRT2, and one 21-mer

**TABLE 1** Primer sequences used for construction of Sirt2 isoforms, Sirt2.1 DN, Sirt2 shRNA, shControl, HBx, and hNTCP and for Sirt2 RT-PCR

Plasmid	Sequence (5'–3')
<b>Sirt2 isoforms</b>	
3×FLAG-tagged Sirt2.1	
Forward	ATGCAAGCCTATGGACTTCTGCGGAAC—
Reverse	ATGCCAATTCTCACTGGGGTTTCTCCCT
3×FLAG-tagged Sirt2.2	
Forward	ATGCAAGCTTATGGACTTCTGCG
Reverse	ATGCCAATTCTCACTGGGGTTTCTCCCT—
3×FLAG-tagged Sirt2.5	
Forward	ATGCAAGCTTATGGCAGAGCCAGA
Reverse	ATGCCAATTCTCACTGGGGTTTCTCCCT—
<b>Sirt2 mutant</b>	
3×FLAG-tagged Sirt2.1 DN	
Forward	TTGGTGGAGGCGTACGGCACCTTCTAC
Reverse	GTAGAAGGTGCCGTACGCCTCCACCAA
<b>shRNAs</b>	
shSIRT2-#1	GCTAAGCTGGATGAAAGAGAA
shSIRT2-#2	GCCAACCATCTGCTCACTACTT
shSIRT2-#3	CCTGCTCATCAACAAGGAGAA
shSIRT2-#4	GCCATCTTTGAGATCAGCTAT
shControl	GCAACAAGATGAAGAGCACCAA
<b>HBV promoters and enhancers</b>	
EnhI/Xp	
Forward	CGGGCTCGAGATGTATACAAGCTAAAC
Reverse	AATGCCAAGCTTGAAACGATG
EnhII/Cp	
Forward	ATGCCTCGAGTCTGCCAAGGTCT
Reverse	ATGCAAGCTTACTTCTTATAAGGG
preS1p	
Forward	CGGGCTCGAGATCAGGTAGTTAATC
Reverse	AATGCCAAGCTTAGAATATGGTGAC
preS2p	
Forward	CGGGCTCGAGCAACAATCCAGATTG
Reverse	AATGCCAAGCTTACTGCCGATTG
<b>HBx</b>	
HA-HBx	
Forward	ATGCTGGCCATGGCTGCTAGGTTG
Reverse	ATGCGAATTCTTAGGCAGAGGTGA
<b>hNTCP</b>	
pCDH-hNTCP-C9	
Forward	AGATTGGAAGCCACCATGGAGGCCACAAC
Reverse	ATTAGCGGCCGCTAAGCGGGCGCCAC
<b>Sirt2</b>	
Forward	ATGGACTTCTGCGGAACCTA
Reverse	GCCCGGCTATTCGCTCCAGGG

RNA (random RNA) was selected as a control. The sequences of shSIRT2-#1, shSIRT2-#2, shSIRT2-#3, shSIRT2-#4, and control shRNA are listed in Table 1. To perform the luciferase reporter assay to examine HBV transcription, luciferase reporter vectors containing the respective enhancers and/or promoters were constructed. The primers used to amplify the respective enhancers and/or promoters from the HBV (adwR9) backbone are listed in Table 1. HA-HBx WT was constructed by PCR-generated amplification of a HBx sequence (Table 1). All constructs were sequenced to confirm the presence of specific mutations and the absence of extraneous mutations.

**Cell culture, DNA transfection, and core particle immunoblotting.** Huh7, HepG2, HepG2-hNTCP-C9, and HEK293T cells were maintained in Dulbecco's modified Eagle's medium (DMEM) supplemented with 1% penicillin-streptomycin and 10% fetal bovine serum (FBS; Gibco BRL) in a humidified atmosphere (37°C with 5% CO<sub>2</sub>). HEK293T cells were passaged every second day, and other cells were passaged every third day. HepG2.2.15 cells were grown as described above, with the addition of G418 (0.5 mg/ml) for selection. HepAD38 cells (a kind gift of C. Seeger, Fox Chase Cancer Center) were grown as described above, with the addition of tetracycline (1 μg/ml). Tetracycline was then removed to induce HBV

transcription. To produce the HBV inoculum for the infection experiment, HepAD38 cells were cultured, as described previously (74). For transfection into Huh7 and HEK293T cells, 4  $\mu$ g of the plasmid construct was mixed with 24  $\mu$ g/ $\mu$ l polyethylenimine (PEI; Polysciences) and 200  $\mu$ l of Opti-MEM (Gibco) and poured into  $1 \times 10^6$  Huh7 or HEK293T cells (in 6-cm plates) 24 h after cell seeding. For cotransfection into Huh7 cells ( $1 \times 10^6$ ) in 6-cm culture plates, 4  $\mu$ g of the 3 $\times$ FLAG-Sirt2.1 or DN mutant construct and/or 4  $\mu$ g of the HBV WT or HBV mutant (TP-Y65F and RT-YMHA) construct under the control of the CMV IE promoter or the 1.3-mer construct from HBV WT was mixed with 24  $\mu$ g/ $\mu$ l PEI (Polysciences) and 200  $\mu$ l of Opti-MEM (Gibco) and poured onto the cells 24 h after seeding. For cotransfection into HepG2 cells ( $3 \times 10^6$  cells in 6-cm culture plates), 4  $\mu$ g of the Sirt2.1 or DN mutant construct and/or 4  $\mu$ g of the 1.3-mer from HBV WT or the HBx-deficient mutant was mixed with 32  $\mu$ g/ $\mu$ l PEI and 200  $\mu$ l of Opti-MEM. pcDNA3 was used to adjust the amount of transfected DNA. At 24 h posttransfection, cell culture medium containing transfected DNA was refreshed, and cells were harvested at 72 h posttransfection. Cells were lysed using 0.2% NP-40 [IGEPAL; Sigma-Aldrich]-TNE (10 mM Tris-HCl [pH 8.0], 50 mM NaCl, 1 mM EDTA) buffer as described previously (37). Next, 4% of the total lysate was electrophoresed in 1% native agarose gels, and resolved core particles were transferred to polyvinylidene fluoride (PVDF) membranes (Millipore). Immunoblotting to visualize core particles was performed using a polyclonal rabbit anti-HBc primary antibody (1:1,000 dilution) (generated in-house) (75), followed by a horseradish peroxidase-conjugated anti-rabbit secondary antibody (1:5,000 dilution) (Thermo Fisher Scientific). Bound secondary antibodies were visualized using enhanced chemiluminescence (ECL Western blotting detection reagent; Amersham). The relative intensities of core particles were measured using ImageJ 1.46r.

**Stable cell lines.** HepG2-hNTCP-C9 stable cells were generated according to previously reported methods (76). A lentiviral expression system was utilized to generate Huh7-, HepG2-, and HepG2-hNTCP-C9-derived Sirt2 knockdown cells. Briefly, HEK293T cells were seeded on 6-cm plates and transfected with 0.5  $\mu$ g of pVSV-G, 1.5  $\mu$ g of pGAG-Pol, and 2  $\mu$ g of the corresponding pSIH1-H1-Puro-shSIRT2 construct (shSIRT2-#1 to -#4) or pSIH1-H1-Puro-shControl in 12  $\mu$ g/ $\mu$ l PEI and 200  $\mu$ l of Opti-MEM. One day after transfection, the medium was changed, and cells were incubated for a further 36 h. The supernatant containing pseudoviral particles and shRNAs was harvested at 2 days posttransfection, and 2 ml of the supernatant and 2 ml of fresh culture medium were mixed and used to infect Huh7, HepG2, or HepG2-hNTCP-C9 cells using 10  $\mu$ g of Polybrene (hexadimethrine bromide; Sigma-Aldrich). Media were changed at 24 h postinfection, and infected cells were reseeded onto new culture plates for selection using 2  $\mu$ g/ml puromycin (Sigma-Aldrich) (for 72 h); this generated Sirt2 knockdown Huh7-shSIRT2-#1 to -#4 and Huh7-shControl cells, HepG2-shSIRT2-#1 to -#4 and HepG2-shControl cells, and HepG2-hNTCP-C9-shSirt2-#2 and -#3 and HepG2-hNTCP-C9-shControl cells.

**Northern, Southern, and nucleic acid blotting.** To analyze HBV RNA expression by Northern blotting, total RNA was extracted from Huh7 and HepG2 cells using TRIzol reagent (catalog number 15596026; Ambion, Invitrogen), according to the manufacturer's instructions. Total RNA (20  $\mu$ g) was denatured at 65°C for 10 min and electrophoresed on 1.2% agarose gels (ultrapure agarose, catalog number 16500500; Invitrogen) containing formaldehyde (catalog number F8775; Sigma-Aldrich) and  $1 \times$  morpholinepropanesulfonic acid (MOPS) buffer (200 mM MOPS, 10 mM EDTA, 50 mM sodium acetate [pH 7]). RNA was then transferred to a nylon membrane (catalog number 11417240001; Roche, Sigma-Aldrich) and hybridized at 68°C for 4 h to a  $^{32}$ P-labeled random-primed probe specific for the full-length HBV sequence. Sirt2 RNA expression was also analyzed by Northern blotting using a  $^{32}$ P-labeled random-primed probe specific for the Sirt2 sequence. To analyze HBV DNA synthesis by Southern blotting, HBV DNA extracted from isolated core particles was separated on agarose gels, transferred to nylon membranes (catalog number 10416296; Whatman), and hybridized to a  $^{32}$ P-labeled random-primed probe specific for full-length HBV, as described previously (37). To analyze nucleic acid inside core particles of HBV, nucleic acid blotting was performed on the same polyvinylidene difluoride (PVDF) membranes used for the detection of core particles. Briefly, the PVDF membranes were treated for 10 s with 0.2 N NaOH and quickly washed with distilled water. Membranes were then dried and hybridized with a  $^{32}$ P-labeled random-primed probe specific for the full-length HBV sequence.

**SDS-PAGE and Western blotting.** Equal quantities (measured by a Bradford assay [77]) of the cell lysate (0.2% NP-40 [IGEPAL; Sigma-Aldrich]-TNE) were subjected to sodium dodecyl sulfate-polyacrylamide gel electrophoresis (SDS-PAGE) on 10% gels. Resolved proteins were then transferred to PVDF membranes and incubated with the appropriate primary antibodies (rabbit polyclonal anti-HBc [1:1,000], rabbit polyclonal anti-HBs [1:1,000] [catalog number 1811; Virostat Inc.], mouse monoclonal anti-FLAG M2 [1:1,000] [catalog number F1804; Sigma], polyclonal rabbit anti-Sirt2 [H-95] [1:1,000] [catalog number sc-20966; Santa Cruz], rabbit polyclonal anti-HDAC6 [1:1,000] [catalog number sc-11420; Santa Cruz], mouse monoclonal anti-glyceraldehyde-3-phosphate dehydrogenase [GAPDH] [1:5,000] [catalog number sc-32233; Santa Cruz], mouse monoclonal anti- $\alpha$ -tubulin [TU-02] [1:5,000] [catalog number sc-8035; Santa Cruz], monoclonal anti-acetylated  $\alpha$ -tubulin clone 6-11B-1 [1:1,000] [catalog number T 6793; Sigma-Aldrich], rabbit polyclonal anti-H3 [1:5,000] [catalog number ab1791; Abcam], mouse monoclonal anti-HA [HA.C5] [1:1,000] [catalog number ab18181; Abcam], mouse monoclonal anti-GSK-3 $\beta$  [1:1,000] [catalog number 11B9; Santa Cruz], rabbit monoclonal anti-phospho-GSK-3 $\beta$  [Ser 9] [1:1,000] [catalog number 9336; Cell Signaling Technology], rabbit monoclonal anti- $\beta$ -catenin [1:1,000] [catalog number D10A8; Cell Signaling Technology], rabbit monoclonal anti-phospho- $\beta$ -catenin [S552] [1:1,000] [catalog number D8E11; Cell Signaling Technology], rabbit polyclonal anti-AKT [1:1,000] [catalog number 9272S; Cell Signaling Technology], rabbit anti-phospho-AKT [T308] [1:1,000] [catalog number 9275S; Cell Signaling Technology], rabbit anti-phospho-AKT [S473] [1:1,000] [catalog number 9271S; Cell Signaling Technology], or mouse anti-rhodopsin monoclonal anti-C9 [1:1,000] [catalog number

MAB5356; Millipore]), followed by anti-rabbit secondary antibodies coupled to horseradish peroxidase (1:5,000 dilution) (Thermo Fisher Scientific) or anti-mouse secondary antibodies coupled to horseradish peroxidase (1:5,000 dilution) (Thermo Fisher Scientific). The blots were then visualized by ECL. The relative band intensities were measured using ImageJ 1.46r.

**AGK2 treatment.** To examine the effects of a Sirt2 inhibitor on HBV replication, AGK2 (catalog number A8231; Sigma-Aldrich) (45) was dissolved in dimethyl sulfoxide (DMSO). In brief, Huh7 or HepG2 cells were seeded onto 6-cm plates and transiently transfected with 4  $\mu$ g of 1.3-mer HBV WT (ayw) or 4  $\mu$ g of 1.3-mer HBV WT (ayw) plus 4  $\mu$ g of the 3 $\times$ FLAG-Sirt2.1 construct (as described above). Cells were exposed to 10  $\mu$ M AGK2 at the time of transfection. Lysates were prepared at both 72 h posttransfection and posttreatment. Cytotoxic effects of AGK2 were determined by an MTT assay, as described previously (78).

**Entecavir and lamivudine treatment.** To examine endogenous Sirt2 expression upon HBV DNA synthesis, the RT-inhibiting nucleoside analogs entecavir (catalog number SML1103; Sigma-Aldrich) and lamivudine (catalog number L1295; Sigma-Aldrich) were dissolved in phosphate-buffered saline (PBS). HepG2 cells on 6-cm plates were transiently transfected with 4  $\mu$ g of 1.3-mer HBV WT (ayw) (as described above). At 24 h posttransfection, the cells were treated with 1  $\mu$ M entecavir or 5  $\mu$ M lamivudine for 48 h. Lysates were prepared at 72 h posttransfection. HepG2-hNTCP-C9 cells were seeded on 6-well plates, and infection was performed as described below (see "HBV preparation and infection"). Cells were treated with 1  $\mu$ M entecavir on the day of infection or 1 day after infection.

**RT-PCR.** To analyze Sirt2 mRNA expression by RT-PCR, total RNA was extracted as described above (see "Northern, Southern, and nucleic acid blotting"). cDNA was synthesized from the extracted RNA (1  $\mu$ g) using oligo(dT) and RevertAid RT (catalog number EP0739; Fermentas), and PCR was then performed using Sirt2 primers (Table 1), amplifying 420 bp of the Sirt2 DNA fragment. The amplified DNA amount was analyzed by using Quantity One software (Bio-Rad) and ImageJ 1.46r.

**Coimmunoprecipitation.** Huh7 cells were transfected with pcDNA3 and the 3 $\times$ FLAG-tagged Sirt2.1 construct or with the 1.3-mer HBV WT (ayw) plus the 3 $\times$ FLAG-tagged Sirt2.1 construct. Cells were harvested 3 days after transfection. To determine the physical interaction between AKT and Sirt2, cell lysates were immunoprecipitated with mouse monoclonal anti-FLAG M2 and immunoblotted with rabbit polyclonal anti-AKT antibodies. Mouse normal IgG (catalog number 12-371; Merck Millipore) was used as a negative control for immunoprecipitation. The lysates were subjected to SDS-PAGE on 10% gels and then transferred to PVDF membranes for immunoblotting with primary antibodies (anti-FLAG M2, anti-GAPDH, and anti-AKT), followed by anti-mouse or anti-rabbit secondary antibodies coupled to horseradish peroxidase. Immunoblots were visualized by enhanced chemiluminescence (ECL Western blotting detection reagent; Amersham).

**HBV preparation and infection.** The HBV inoculum for infection was harvested from HepAD38 cells as described previously, with minor modifications (74, 79). Briefly, cells were grown in GlutaMAX DMEM supplemented with 10% FBS, 0.5 mg/ml G418, 50  $\mu$ M hydrocortisone hemisuccinate, 5  $\mu$ g/ml insulin, and 1% penicillin-streptomycin. The culture supernatant collected every third day from days 10 to 31 was concentrated by 20 to 60% discontinuous sucrose gradient ultracentrifugation (Optima L-90K; Beckman Coulter). HBV DNA in the precipitant was quantitated by Southern blotting. For HBV infection,  $2 \times 10^5$  HepG2, HepG2-hNTCP-C9-shControl, HepG2-hNTCP-C9-shSirt2-#2, and HepG2-hNTCP-C9-shSirt2-#3 cells were seeded in collagen-coated (catalog number 354249; Corning) 6-well plates and infected with HBV at  $1.7 \times 10^3$  genome equivalents (GEq) per cell in medium containing 4% polyethylene glycol (catalog number 25322-68-3; Affymetrix), as described previously (80). One day after infection, the cells were washed thoroughly with PBS to remove the residual HBV and were maintained in the same medium containing 2.5% dimethyl sulfoxide, as described previously (80). The medium was changed every other day. For Northern blot analysis, total cell lysates were prepared at 5 days postinfection. Lysates were prepared at 9 days postinfection and subjected to SDS-PAGE and immunoblotting, core particle immunoblotting, and Southern blot analysis as described above.

**Fractionation of Sirt2 isoforms and HDAC6.** HEK293T cells were transfected with 4  $\mu$ g of the respective Sirt2 isoforms or a HDAC6-encoding vector as described above (see "Cell culture, DNA transfection, and core particle immunoblotting"). At 24, 36, and 72 h posttransfection, cells were harvested and resuspended in 200  $\mu$ l of cold harvest buffer (10 mM HEPES [pH 7.9], 50 mM NaCl, 0.5 M sucrose, 0.1 mM EDTA, 0.5% Triton X-100, 10 mM NaF, and freshly added 1 mM dithiothreitol [DTT]). The cytoplasmic and nuclear fractions were prepared according to the Genetex protocol for fractionation of membrane/cytoplasmic and nuclear proteins. Briefly, pelleted nuclei from total cell lysates were prepared by centrifugation at  $1,200 \times g$  in a swinging-bucket rotor for 10 min. The supernatant was transferred to a new tube and cleared at 13,000 rpm for 15 min to obtain cytoplasmic and membrane proteins. Next, 4 volumes of buffer C (10 mM HEPES [pH 7.9], 500 mM NaCl, 0.1 mM EDTA, 0.1 mM EGTA, 0.1% NP-40) were added to the nuclear pellet and vortexed for 15 min at 4°C, and the nuclei were pelleted at 13,000 rpm for 10 min at 4°C. The supernatant from the nuclear extract was transferred to a new tube.

**Luciferase reporter assay.** HepG2 or Huh7 cells were cotransfected with the luciferase report vector (2  $\mu$ g) pGL3-null, pGL3-EnhI/Xp, pGL3-EnhII/Cp, pGL3-PreS1p, or pGL3-PreS2p plus 2  $\mu$ g of 3 $\times$ FLAG-Sirt2.1 or pcDNA3.1. pGL3-EnhI/Xp, pGL3-EnhII/Cp, pGL3-PreS1p, or pGL3-PreS2p was transfected into shSIRT2-#2 and shSIRT2-#3 KD Huh7 cells. After 72 h, cells were lysed using 5 $\times$  luciferase cell culture lysis reagent (catalog number E153A; Promega), and luciferase activity was analyzed using luciferin (Promega) and a luminometer (Molecular Devices).

**Statistical analysis.** Data are expressed as the means  $\pm$  standard deviations. Mean values were compared using Student's *t* test. *P* values of <0.05 were considered statistically significant.

## ACKNOWLEDGMENTS

This work was supported by National Research Foundation grants, funded by the South Korean Government (NRF-2015R1D1A1A01057259).

## REFERENCES

- Summers J, Mason WS. 1982. Replication of the genome of a hepatitis B-like virus by reverse transcription of an RNA intermediate. *Cell* 29: 403–415. [https://doi.org/10.1016/0092-8674\(82\)90157-X](https://doi.org/10.1016/0092-8674(82)90157-X).
- Yan H, Zhong G, Xu G, He W, Jing Z, Gao Z, Huang Y, Qi Y, Peng B, Wang H, Fu L, Song M, Chen P, Gao W, Ren B, Sun Y, Cai T, Feng X, Sui J, Li W. 2012. Sodium taurocholate cotransporting polypeptide is a functional receptor for human hepatitis B and D virus. *Elife* 1:e00049. <https://doi.org/10.7554/eLife.00049>.
- Kann M, Schmitz A, Rabe B. 2007. Intracellular transport of hepatitis B virus. *World J Gastroenterol* 13:39–47. <https://doi.org/10.3748/wjg.v13.i1.39>.
- Köck J, Rösler C, Zhang JJ, Blum HE, Nassal M, Thoma C. 2010. Generation of covalently closed circular DNA of hepatitis B viruses via intracellular recycling is regulated in a virus specific manner. *PLoS Pathog* 6:e1001082. <https://doi.org/10.1371/journal.ppat.1001082>.
- Locarnini S. 2004. Molecular virology of hepatitis B virus. *Semin Liver Dis* 24(Suppl 1):3–10. <https://doi.org/10.1055/s-2004-828672>.
- Ringelhan M, O'Connor T, Protzer U, Heikenwalder M. 2015. The direct and indirect roles of HBV in liver cancer: prospective markers for HCC screening and potential therapeutic targets. *J Pathol* 235:355–367. <https://doi.org/10.1002/path.4434>.
- de Ruijter AJ, van Gennip AH, Caron HN, Kemp S, van Kuilenburg AB. 2003. Histone deacetylases (HDACs): characterization of the classical HDAC family. *Biochem J* 370:737–749. <https://doi.org/10.1042/bj20021321>.
- Finnin MS, Donigan JR, Pavletich NP. 2001. Structure of the histone deacetylase SIRT2. *Nat Struct Biol* 8:621–625. <https://doi.org/10.1038/89668>.
- North BJ, Verdin E. 2004. Sirtuins: Sir2-related NAD-dependent protein deacetylases. *Genome Biol* 5:224. <https://doi.org/10.1186/gb-2004-5-5-224>.
- Blander G, Guarente L. 2004. The Sir2 family of protein deacetylases. *Annu Rev Biochem* 73:417–435. <https://doi.org/10.1146/annurev.biochem.73.011303.073651>.
- Frye RA. 2000. Phylogenetic classification of prokaryotic and eukaryotic Sir2-like proteins. *Biochem Biophys Res Commun* 273:793–798. <https://doi.org/10.1006/bbrc.2000.3000>.
- Ren JH, Tao Y, Zhang ZZ, Chen WX, Cai XF, Chen K, Ko BC, Song CL, Ran LK, Li WY, Huang AL, Chen J. 2014. Sirtuin 1 regulates hepatitis B virus transcription and replication by targeting transcription factor AP-1. *J Virol* 88:2442–2451. <https://doi.org/10.1128/JVI.02861-13>.
- Ren JH, Chen X, Zhou L, Tao NN, Zhou HZ, Liu B, Li WY, Huang AL, Chen J. 2016. Protective role of sirtuin3 (SIRT3) in oxidative stress mediated by hepatitis B virus X protein expression. *PLoS One* 11:e0150961. <https://doi.org/10.1371/journal.pone.0150961>.
- Wang J, Koh HW, Zhou L, Bae UJ, Lee HS, Bang IH, Ka SO, Oh SH, Bae EJ, Park BH. 2017. Sirtuin 2 aggravates posts ischemic liver injury by deacetylating mitogen-activated protein kinase phosphatase-1. *Hepatology* 65: 225–236. <https://doi.org/10.1002/hep.28777>.
- Arteaga M, Shang N, Ding X, Yong S, Cotler SJ, Denning MF, Shimamura T, Breslin P, Lüscher B, Qiu W. 2016. Inhibition of SIRT2 suppresses hepatic fibrosis. *Am J Physiol Gastrointest Liver Physiol* 310: G1155–G1168. <https://doi.org/10.1152/ajpgi.00271.2015>.
- Chen J, Chan AW, To KF, Chen W, Zhang Z, Ren J, Song C, Cheung YS, Lai PB, Cheng SH, Ng MH, Huang A, Ko BC. 2013. SIRT2 overexpression in hepatocellular carcinoma mediates epithelial to mesenchymal transition by protein kinase B/glycogen synthase kinase-3 $\beta$ / $\beta$ -catenin signaling. *Hepatology* 57:2287–2298. <https://doi.org/10.1002/hep.26278>.
- Xie HJ, Jung KH, Nam SW. 2011. Overexpression of Sirt2 contributes tumor cell growth in hepatocellular carcinoma. *Mol Cell Toxicol* 7:367–374. <https://doi.org/10.1007/s13273-011-0046-5>.
- Cheng ST, Ren JH, Cai XF, Jiang H, Chen J. 2018. HBx-elevated SIRT2 promotes HBV replication and hepatocarcinogenesis. *Biochem Biophys Res Commun* 496:904–910. <https://doi.org/10.1016/j.bbrc.2018.01.127>.
- Rothgiesser KM, Erenner S, Waibel S, Luscher B, Hottiger MO. 2010. SIRT2 regulates NF- $\kappa$ B dependent gene expression through deacetylation of p65 Lys310. *J Cell Sci* 123:4251–4258. <https://doi.org/10.1242/jcs.073783>.
- Wang F, Chan CH, Chen K, Guan X, Lin HK, Tong Q. 2012. Deacetylation of FOXO3 by SIRT1 or SIRT2 leads to Skp2-mediated FOXO3 ubiquitination and degradation. *Oncogene* 31:1546–1557. <https://doi.org/10.1038/onc.2011.347>.
- Bosch-Presegué L, Vaquero A. 2011. The dual role of sirtuins in cancer. *Genes Cancer* 2:648–662. <https://doi.org/10.1177/1947601911417862>.
- North BJ, Marshall BL, Borra MT, Denu JM, Verdin E. 2003. The human Sir2 ortholog, SIRT2, is an NAD<sup>+</sup>-dependent tubulin deacetylase. *Mol Cell* 11:437–444. [https://doi.org/10.1016/S1097-2765\(03\)00038-8](https://doi.org/10.1016/S1097-2765(03)00038-8).
- Kim HS, Vassilopoulos A, Wang RH, Lahusen T, Xiao Z, Xu X, Li C, Veenstra TD, Li B, Yu H, Ji J, Wang XW, Park SH, Cha YI, Gius D, Deng CX. 2011. SIRT2 maintains genome integrity and suppresses tumorigenesis through regulating APC/C activity. *Cancer Cell* 20:487–499. <https://doi.org/10.1016/j.ccr.2011.09.004>.
- Hiratsuka M, Inoue T, Toda T, Kimura N, Shirayoshi Y, Kamitani H, Watanabe T, Ohama E, Tahimic CG, Kurimasa A, Oshimura M. 2003. Proteomics-based identification of differentially expressed genes in human gliomas: down-regulation of SIRT2 gene. *Biochem Biophys Res Commun* 309:558–566. <https://doi.org/10.1016/j.bbrc.2003.08.029>.
- Ramakrishnan G, Davaakhuu G, Kaplun L, Chung WC, Rana A, Atfi A, Miele L, Tzivion G. 2014. Sirt2 deacetylase is a novel AKT binding partner critical for AKT activation by insulin. *J Biol Chem* 289:6054–6066. <https://doi.org/10.1074/jbc.M113.537266>.
- Boyault S, Rickman DS, de Reyniès A, Balabaud C, Rebouissou S, Jeannot E, Héroult A, Saric J, Belghiti J, Franco D, Bioulac-Sage P, Laurent-Puig P, Zucman-Rossi J. 2007. Transcriptome classification of HCC is related to gene alterations and to new therapeutic targets. *Hepatology* 45:42–52. <https://doi.org/10.1002/hep.21467>.
- Courtney KD, Corcoran RB, Engelman JA. 2010. The PI3K pathway as drug target in human cancer. *J Clin Oncol* 28:1075–1083. <https://doi.org/10.1200/JCO.2009.25.3641>.
- Engelman JA. 2009. Targeting PI3K signalling in cancer: opportunities, challenges and limitations. *Nat Rev Cancer* 9:550–562. <https://doi.org/10.1038/nrc2664>.
- Rawat S, Bouchard MJ. 2015. The hepatitis B virus (HBV) HBx protein activates AKT to simultaneously regulate HBV replication and hepatocyte survival. *J Virol* 89:999–1012. <https://doi.org/10.1128/JVI.02440-14>.
- Cooray S. 2004. The pivotal role of phosphatidylinositol 3-kinase-Akt signal transduction in virus survival. *J Gen Virol* 85:1065–1076. <https://doi.org/10.1099/vir.0.19771-0>.
- Caron C, Col E, Khochbin S. 2003. The viral control of cellular acetylation signaling. *Bioessays* 25:58–65. <https://doi.org/10.1002/bies.10202>.
- Jeng MY, Ali I, Ott M. 2015. Manipulation of the host protein acetylation network by human immunodeficiency virus type 1. *Crit Rev Biochem Mol Biol* 50:314–325. <https://doi.org/10.3109/10409238.2015.1061973>.
- Husain M, Cheung CY. 2014. Histone deacetylase 6 inhibits influenza A virus release by downregulating the trafficking of viral components to the plasma membrane via its substrate, acetylated microtubules. *J Virol* 88:11229–11239. <https://doi.org/10.1128/JVI.00727-14>.
- Roohvand F, Maillard P, Lavergne JP, Boulant S, Walic M, Andréo U, Goueslain J, Helle F, Mallet A, McLauchlan J, Budkowska A. 2009. Initiation of hepatitis C virus infection requires the dynamic microtubule network: role of the viral nucleocapsid protein. *J Biol Chem* 284: 13778–13791. <https://doi.org/10.1074/jbc.M807873200>.
- Ladner SK, Otto MJ, Barker CS, Zaifert K, Wang GH, Guo JT, Seeger C, King RW. 1997. Inducible expression of human hepatitis B virus (HBV) in stably transfected hepatoblastoma cells: a novel system for screening potential inhibitors of HBV replication. *Antimicrob Agents Chemother* 41:1715–1720.
- Sells MA, Chen ML, Acs G. 1987. Production of hepatitis B virus particles in Hep G2 cells transfected with cloned hepatitis B virus DNA. *Proc Natl Acad Sci U S A* 84:1005–1009.
- Kim HY, Park GS, Kim EG, Kang SH, Shin HJ, Park S, Kim KH. 2004. Oligomer synthesis by priming deficient polymerase in hepatitis B virus

- core particle. *Virology* 322:22–30. <https://doi.org/10.1016/j.virol.2004.01.009>.
38. Chang LJ, Hirsch RC, Ganem D, Varmus HE. 1990. Effects of insertional and point mutations on the functions of duck hepatitis B virus polymerase. *J Virol* 64:5553–5558.
  39. Doong SL, Tsai CH, Schinazi RF, Liotta DC, Cheng YC. 1991. Inhibition of the replication of hepatitis B virus in vitro by 2',3'-dideoxy-3'-thiacytidine and related analogues. *Proc Natl Acad Sci U S A* 88:8495–8499.
  40. Abdelhamed AM, Kelley CM, Miller TG, Furman PA, Cable EE, Isom HC. 2003. Comparison of anti-hepatitis B virus activities of lamivudine and clevudine by a quantitative assay. *Antimicrob Agents Chemother* 47:324–336. <https://doi.org/10.1128/AAC.47.1.324-336.2003>.
  41. North BJ, Verdin E. 2007. Interphase nucleo-cytoplasmic shuttling and localization of SIRT2 during mitosis. *PLoS One* 2:e784. <https://doi.org/10.1371/journal.pone.0000784>.
  42. Rack JG, VanLinden MR, Lutter T, Aasland R, Ziegler M. 2014. Constitutive nuclear localization of an alternatively spliced sirtuin-2 isoform. *J Mol Biol* 426:1677–1691. <https://doi.org/10.1016/j.jmb.2013.10.027>.
  43. Hubbert C, Guardiola A, Shao R, Kawaguchi Y, Ito A, Nixon A, Yoshida M, Wang XF, Yao TP. 2002. HDAC6 is a microtubule-associated deacetylase. *Nature* 417:455–458. <https://doi.org/10.1038/417455a>.
  44. Dryden SC, Nahhas FA, Nowak JE, Goustin AS, Tainsky MA. 2003. Role for human SIRT2 NAD<sup>+</sup>-dependent deacetylase activity in control of mitotic exit in the cell cycle. *Mol Cell Biol* 23:3173–3185. <https://doi.org/10.1128/MCB.23.9.3173-3185.2003>.
  45. Outeiro TF, Kontopoulos E, Altmann SM, Kufareva I, Strathearn KE, Amore AM, Volk CB, Maxwell MM, Rochet JC, McLean PJ, Young AB, Abagyan R, Feany MB, Hyman BT, Kazantsev AG. 2007. Sirtuin 2 inhibitors rescue alpha-synuclein-mediated toxicity in models of Parkinson's disease. *Science* 317:516–519. <https://doi.org/10.1126/science.1143780>.
  46. Lee YI, Kang-Park S, Do SI, Lee YI. 2001. The hepatitis B virus-X protein activates a phosphatidylinositol 3-kinase-dependent survival signaling cascade. *J Biol Chem* 276:16969–16977. <https://doi.org/10.1074/jbc.M011263200>.
  47. Ding Q, Xia W, Liu JC, Yang JY, Lee DF, Xia J, Bartholomeusz G, Li Y, Pan Y, Li Z, Bargou RC, Qin J, Lai CC, Tsai FJ, Tsai CH, Hung MC. 2005. Erk associates with and primes GSK-3beta for its inactivation resulting in upregulation of beta-catenin. *Mol Cell* 19:159–170. <https://doi.org/10.1016/j.molcel.2005.06.009>.
  48. Cha MY, Kim CM, Park YM, Ryu WS. 2004. Hepatitis B virus X protein is essential for the activation of Wnt/beta-catenin signaling in hepatoma cells. *Hepatology* 39:1683–1693. <https://doi.org/10.1002/hep.20245>.
  49. Hsieh A, Kim HS, Lim SO, Yu DY, Jung G. 2011. Hepatitis B viral X protein interacts with tumor suppressor adenomatous polyposis coli to activate Wnt/beta-catenin signaling. *Cancer Lett* 300:162–172. <https://doi.org/10.1016/j.canlet.2010.09.018>.
  50. Melegari M, Wolf SK, Schneider RJ. 2005. Hepatitis B virus DNA replication is coordinated by core protein serine phosphorylation and HBx expression. *J Virol* 79:9810–9820. <https://doi.org/10.1128/JVI.79.15.9810-9820.2005>.
  51. Bouchard MJ, Wang LH, Schneider RJ. 2001. Calcium signaling by HBx protein in hepatitis B virus DNA replication. *Science* 294:2376–2378. <https://doi.org/10.1126/science.294.5550.2376>.
  52. Yoon S, Jung J, Kim T, Park S, Chwae YJ, Shin HJ, Kim K. 2011. Adiponectin, a downstream target gene of peroxisome proliferator-activated receptor  $\gamma$ , controls hepatitis B virus replication. *Virology* 409:290–298. <https://doi.org/10.1016/j.virol.2010.10.024>.
  53. Bruix J, Gores GJ, Mazzaferro V. 2014. Hepatocellular carcinoma: clinical frontiers and perspectives. *Gut* 63:844–855. <https://doi.org/10.1136/gutjnl-2013-306627>.
  54. Jemal A, Bray F, Center MM, Ferlay JJ, Ward E, Forman D. 2011. Global cancer statistics. *CA Cancer J Clin* 61:69–90. <https://doi.org/10.3322/caac.20107>.
  55. Lara-Pezzi E, Majano PL, Yáñez-Mó M, Gómez-Gonzalo M, Carretero M, Moreno-Otero R, Sánchez-Madrid F, López-Cabrera M. 2001. Effect of the hepatitis B virus HBx protein on integrin-mediated adhesion to and migration on extracellular matrix. *J Hepatol* 34:409–415. [https://doi.org/10.1016/S0168-8278\(00\)00090-8](https://doi.org/10.1016/S0168-8278(00)00090-8).
  56. Huang S, Zhao Z, Tang D, Zhou Q, Li Y, Zhou L, Yin Y, Wang Y, Pan Y, Dorfman RG, Ling T, Zhang M. 2017. Downregulation of SIRT2 inhibits invasion of hepatocellular carcinoma by inhibiting energy metabolism. *Transl Oncol* 10:917–927. <https://doi.org/10.1016/j.tranon.2017.09.006>.
  57. Kawanaka M, Nishino K, Nakamura J, Oka T, Urata N, Goto D, Suehiro M, Kawamoto H, Kudo M, Yamada G. 2014. Quantitative levels of hepatitis B virus DNA and surface antigen and the risk of hepatocellular carcinoma in patients with hepatitis B receiving long-term nucleos(t)ide analogue therapy. *Liver Cancer* 3:41–52. <https://doi.org/10.1159/000343857>.
  58. Chen CJ, Yang HI, Su J, Jen CL, You SL, Lu SN, Huang GT, Iloeje UH, REVEAL-HBV Study Group. 2006. Risk of hepatocellular carcinoma across a biological gradient of serum hepatitis B virus DNA level. *JAMA* 295:65–73. <https://doi.org/10.1001/jama.295.1.65>.
  59. Yu MW, Yeh SH, Chen PJ, Liaw YF, Lin CL, Liu CJ, Shih WL, Kao JH, Chen DS, Chen JH. 2005. Hepatitis B virus genotype and DNA level and hepatocellular carcinoma: a prospective study in men. *J Natl Cancer Inst* 97:265–272. <https://doi.org/10.1093/jnci/dji043>.
  60. Yang WJ, Chang CJ, Yeh SH, Lin WH, Wang SH, Tsai TF, Chen DS, Chen PJ. 2009. Hepatitis B virus X protein enhances the transcriptional activity of the androgen receptor through c-Src and glycogen synthase kinase-3beta kinase pathways. *Hepatology* 49:1515–1524. <https://doi.org/10.1002/hep.22833>.
  61. Deng JJ, Kong KE, Gao WW, Tang HV, Chaudhary V, Cheng Y, Zhou J, Chan CP, Wong DK, Yuen MF, Jin DY. 2017. Interplay between SIRT1 and hepatitis B virus X protein in the activation of viral transcription. *Biochim Biophys Acta* 1860:491–501. <https://doi.org/10.1016/j.bbaprm.2017.02.007>.
  62. Srisuttee R, Koh SS, Kim SJ, Malilas W, Boonying W, Cho IR, Jhun BH, Ito M, Horio Y, Seto E, Oh S, Chung YH. 2012. Hepatitis B virus X (HBX) protein upregulates  $\beta$ -catenin in a human hepatic cell line by sequestering SIRT1 deacetylase. *Oncol Rep* 28:276–282. <https://doi.org/10.3892/or.2012.1798>.
  63. Koyuncu E, Budayeva HG, Miteva YV, Ricci DP, Silhavy TJ, Shenk T, Cristea IM. 2014. Sirtuins are evolutionarily conserved viral restriction factors. *mBio* 5:e02249-14. <https://doi.org/10.1128/mBio.02249-14>.
  64. Etienne-Manneville S. 2010. From signaling pathways to microtubule dynamics: the key players. *Curr Opin Cell Biol* 22:104–111. <https://doi.org/10.1016/j.ceb.2009.11.008>.
  65. Choudhary C, Kumar C, Gnäd F, Nielsen ML, Rehman M, Walther TC, Olsen JV, Mann M. 2009. Lysine acetylation targets protein complexes and co-regulates major cellular functions. *Science* 325:834–840. <https://doi.org/10.1126/science.1175371>.
  66. Fukushima N, Furuta D, Hidaka Y, Moriyama R, Tsujiuchi T. 2009. Post-translational modifications of tubulin in the nervous system. *J Neurochem* 109:683–693. <https://doi.org/10.1111/j.1471-4159.2009.06013.x>.
  67. Naranatt PP, Krishnan HH, Smith MS, Chandran B. 2005. Kaposi's sarcoma-associated herpesvirus modulates microtubule dynamics via 519 RhoA-GTP-diaphanous 2 signaling and utilizes the dynein motors to deliver its DNA to the nucleus. *J Virol* 79:1191–1206. <https://doi.org/10.1128/JVI.79.2.1191-1206.2005>.
  68. Warren JC, Rutkowski A, Cassimeris L. 2006. Infection with replication-deficient adenovirus induces changes in the dynamic instability of host cell microtubules. *Mol Biol Cell* 17:3557–3568. <https://doi.org/10.1091/mbc.e05-09-0850>.
  69. Husain M, Harrod KS. 2011. Enhanced acetylation of alpha-tubulin in influenza A virus infected epithelial cells. *FEBS Lett* 585:128–132. <https://doi.org/10.1016/j.febslet.2010.11.023>.
  70. Valenzuela-Fernández A, Alvarez S, Gordon-Alonso M, Barrero M, Ursa A, Cabrero JR, Fernández G, Naranjo-Suárez S, Yáñez-Mo M, Serrador JM, Muñoz-Fernández MA, Sánchez-Madrid F. 2005. Histone deacetylase 6 regulates human immunodeficiency virus type 1 infection. *Mol Biol Cell* 16:5445–5454. <https://doi.org/10.1091/mbc.e05-04-0354>.
  71. Sabo Y, Walsh D, Barry DS, Tinaztepe S, de Los Santos K, Goff SP, Gundersen GG, Naghavi MH. 2013. HIV-1 induces the formation of stable microtubules to enhance early infection. *Cell Host Microbe* 14:535–546. <https://doi.org/10.1016/j.chom.2013.10.012>.
  72. Zhang S, Jiang Y, Cheng Q, Zhong Y, Qin Y, Chen M. 2017. Inclusion body formation of human parainfluenza virus type 3 regulated by acetylated  $\alpha$ -tubulin enhances viral replication. *J Virol* 91:e01802-16. <https://doi.org/10.1128/JVI.01802-16>.
  73. Han Y, Jin YH, Kim YJ, Kang BY, Choi HJ, Kim DW, Yeo CY, Lee KY. 2008. Acetylation of Sirt2 by p300 attenuates its deacetylase activity. *Biochem Biophys Res Commun* 375:576–580. <https://doi.org/10.1016/j.bbrc.2008.08.042>.
  74. Watashi K, Liang G, Iwamoto M, Marusawa H, Uchida N, Daito T, Kitamura K, Muramatsu M, Ohashi H, Kiyohara T, Suzuki R, Li J, Tong S, Tanaka Y, Murata K, Aizaki H, Wakita T. 2013. Interleukin-1 and tumor necrosis factor- $\alpha$  trigger restriction of hepatitis B virus infection via a cytidine

- deaminase activation-induced cytidine deaminase (AID). *J Biol Chem* 288:31715–31727. <https://doi.org/10.1074/jbc.M113.501122>.
75. Jung J, Kim HY, Kim T, Shin BH, Park GS, Park S, Chwae YJ, Shin HJ, Kim K. 2012. C-terminal substitution of HBV core proteins with those from DHBV reveals that arginine-rich 167RRRSQSPRR175 domain is critical for HBV replication. *PLoS One* 7:e41087. <https://doi.org/10.1371/journal.pone.0041087>.
76. Nkongolo S, Ni Y, Lempp FA, Kaufman C, Lindner T, Esser-Nobis K, Lohmann V, Mier W, Mehrle S, Urban S. 2014. Cyclosporin A inhibits hepatitis B and hepatitis D virus entry by cyclophilin-independent interference with the NTCP receptor. *J Hepatol* 60:723–731. <https://doi.org/10.1016/j.jhep.2013.11.022>.
77. Bradford MM. 1976. A rapid and sensitive method for the quantitation of microgram quantities of protein utilizing the principle of protein-dye binding. *Anal Biochem* 72:248–254. [https://doi.org/10.1016/0003-2697\(76\)90527-3](https://doi.org/10.1016/0003-2697(76)90527-3).
78. Jung J, Kim NK, Park S, Shin HJ, Hwang SG, Kim K. 2015. Inhibitory effect of *Phyllanthus urinaria* L. extract on the replication of lamivudine-resistant hepatitis B virus in vitro. *BMC Complement Altern Med* 15:255. <https://doi.org/10.1186/s12906-015-0792-3>.
79. Ko C, Lee S, Windisch MP, Ryu WS. 2014. DDX3 DEAD-box RNA helicase is a host factor that restricts hepatitis B virus replication at the transcriptional level. *J Virol* 88:13689–13698. <https://doi.org/10.1128/JVI.02035-14>.
80. Ni Y, Lempp FA, Mehrle S, Nkongolo S, Kaufman C, Fäth M, Stindt J, Königer C, Nassal M, Kubitz R, Sülthmann H, Urban S. 2014. Hepatitis B and D viruses exploit sodium taurocholate co-transporting polypeptide for species-specific entry into hepatocytes. *Gastroenterology* 146:1070–1083. <https://doi.org/10.1053/j.gastro.2013.12.024>.